

**Zeitschrift:** IABSE reports of the working commissions = Rapports des commissions de travail AIPC = IVBH Berichte der Arbeitskommissionen

**Band:** 13 (1973)

**Rubrik:** Theme IV: Experimental studies concerning reinforced, prestressed and partially prestressed concrete structures and their elements

### **Nutzungsbedingungen**

Die ETH-Bibliothek ist die Anbieterin der digitalisierten Zeitschriften. Sie besitzt keine Urheberrechte an den Zeitschriften und ist nicht verantwortlich für deren Inhalte. Die Rechte liegen in der Regel bei den Herausgebern beziehungsweise den externen Rechteinhabern. [Siehe Rechtliche Hinweise.](#)

### **Conditions d'utilisation**

L'ETH Library est le fournisseur des revues numérisées. Elle ne détient aucun droit d'auteur sur les revues et n'est pas responsable de leur contenu. En règle générale, les droits sont détenus par les éditeurs ou les détenteurs de droits externes. [Voir Informations légales.](#)

### **Terms of use**

The ETH Library is the provider of the digitised journals. It does not own any copyrights to the journals and is not responsible for their content. The rights usually lie with the publishers or the external rights holders. [See Legal notice.](#)

**Download PDF:** 04.04.2025

**ETH-Bibliothek Zürich, E-Periodica, <https://www.e-periodica.ch>**

## Behaviour of Reinforced Concrete Beams under Combined Moment and Shear Reversal

Comportement des poutres en béton armé soumises à une inversion combinée du moment et de l'effort de cisaillement

Verhalten von Stahlbetonbalken unter kombinierter Momenten/Querkraft-Wechselbeanspruchung

Mehmet CELEBI

Assistant Professor of Civil Engineering  
Middle East Technical University  
Ankara, Turkey

Joseph PENZIEN

Professor of Structural Engineering  
and Director of Earthquake Engineering Research Center  
University of California  
Berkeley, California, USA

### INTRODUCTION

The behavior of a shear span under repeated reversal of loading has been studied by Brown and Jirsa (1) who concluded that the nonlinear behavior of reinforced concrete beams beyond yield is influenced by both Bauschinger effect and shear deformation. Therefore, it appears that seismic properties such as energy absorption capacity and stiffness degradation of a shear span will be influenced by the magnitude of nominal shear stress applied to the span. Furthermore, this nonlinear behavior will result in the development of regions which become critical during an earthquake due to the excessive inelastic deformations imposed (2). One critical region influenced by both shear and flexural stress is the region in a shear span immediately next to a column. Two shear spans and portions of columns as stubs form an interior component of a multi-story frame. Typical components of this type have been tested previously by others to obtain their force-deformation hysteretic behavior (3,4,5,6).

In this paper, the influence of shear span to depth ratio,  $a/d$ , amount of web reinforcement, and rate of loading on the seismic properties of reinforced concrete beams are examined. The experimental results for 12 specimens tested as simple beams using the component testing facility shown in Fig. 1 are presented.

### EXPERIMENTAL WORK

The testing facility used consists of a test frame and an hydraulically powered and electronically controlled actuator having a load rating of 75 kips statically and 50 kips dynamically and having a displacement range of  $\pm 6$  inches. Ten of the 12 test specimens had a 9"x15" cross section and were reinforced longitudinally with four #7 bars (1.03%). The theoretical flexural capacity of this section is about 750 k-in and its effective depth,  $d$ , is 13 in. The maximum applied nominal shear stress which depended on the  $a/d$  ratio was about  $3.75\sqrt{f'_c}$ . The stirrups used were #3 bars with spacings  $s=3.25$ ", in accordance with the ACI and UBC building codes; i.e.,  $s=d/4$ , and  $s=6$ " (7,8).

To investigate the dynamic properties of these beams, a prescribed triangularly shaped displacement-time signal was used which increased in amplitude after every four cycles of displacement at the same amplitude (Fig. 2). Continuous loading with constant velocity was applied to all the specimens. Initially, each specimen (except beam 1) was subjected to the 20 cycles of loading within the elastic limit. Subsequently, 20 more cycles of loading was applied which deformed the member beyond yield.

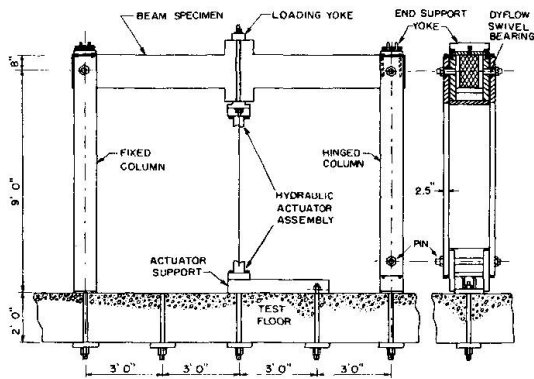


Fig. 1: Test Frame

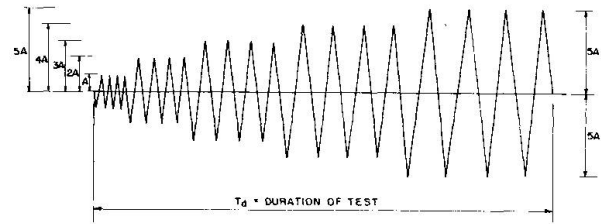


Fig. 2: Load Signal

Various electronic instruments were used to obtain load-deflection, moment-curvature, and steel strain time histories and also to obtain shear-deformation indices. Linear variable differential transformers (LVDT) in conjunction with amplifiers, power supplies and visicorders were used to measure and record all displacements. The displacement and corresponding load applied by the actuator were measured by a built-in LVDT and a load cell, respectively. Whenever possible, X-Y recorders were used to plot the load deflection relationships.

#### TEST RESULTS

Only typical results will be presented herein. In Table 1, certain properties of the beams are presented including yield deflections, yield strengths, maximum applied loads and average nominal shear stresses.

TABLE 1 PROPERTIES OF SPECIMENS AND THEIR APPLIED LOADS

BEAM	a/d	$f'_c$ psi	$f_y$ ksi	s in	$\Delta_y$ in		$F_y$ kips		$F_{max}$ kips		$v_u/\sqrt{f'_c}$ (avg)
					+	-	+	-	+	-	
1	5.10	2640	52.4	6.00	.57	.64	22.8	26.9	23.0	27.5	1.75
2	5.10	4750	52.4	6.00	.48	.50	23.3	24.7	24.0	27.5	1.75
5	5.10	4060	51.8	3.25	.55	.51	25.2	29.5	23.0	28.0	1.75
6	5.10	4060	51.8	3.25	.50	.51	20.8	24.7	23.0	28.0	1.75
7	3.70	4650	51.8	6.00	.35	.33	38.3	36.3	32.0	34.0	2.25
9	3.70	4250	51.8	3.25	.35	.36	37.3	36.6	32.0	36.0	2.25
10	3.70	4250	51.8	3.25	.35	.35	30.3	32.1	32.0	36.0	2.25
11	2.31	4590	50.1	3.25	.22	.21	59.4	59.7	59.0	60.0	3.75
12	2.31	4590	50.1	3.25	.23	.21	57.5	53.2	59.0	60.0	3.75

A typical elastic load-deflection diagram is seen in Fig. 3 for beam No. 6. Load-deflection diagrams for beams Nos. 5, 9, and 12 are seen in Figs. 4, 5 and 6, respectively. A typical moment-curvature diagram is seen in Fig. 7 for beam No. 9. Typical strain histories for the same beam are seen in Fig. 8. Typical shear force-shear deformation index  $\alpha$  is seen in Fig. 9 for beam No. 12. This index is defined as the chord rotation angle calculated from the relative displacements between the stub and a cross section 11" away from its outer face. The instrumentation used and the state of beam No. 12 after testing are seen in Fig. 10.

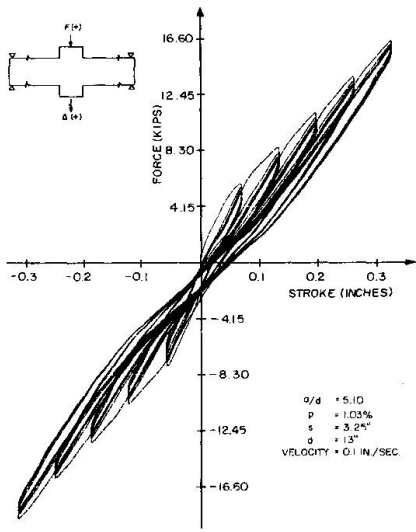


Fig. 3 Elastic Hysteresis Loops (Beam 6)

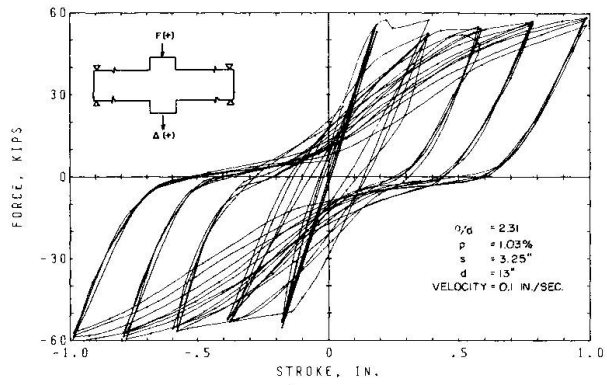


Fig. 6 Inelastic  $F - \Delta$  Hysteresis Loops

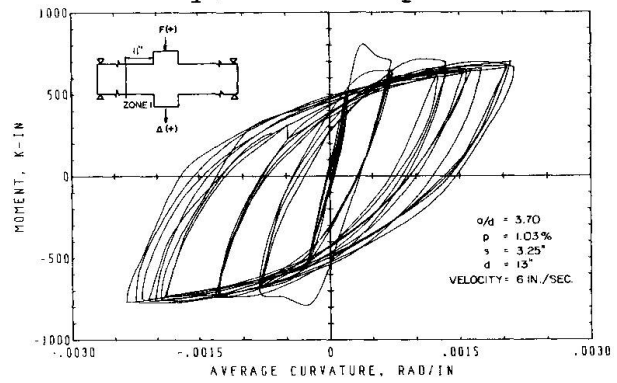


Fig. 7  $M - \psi$  Hysteresis Loops (Beam 9)

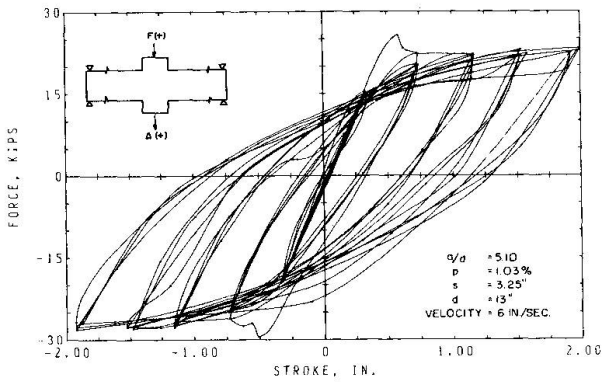


Fig. 4 Inelastic  $F - \Delta$  Hysteresis Loops (Beam 5)

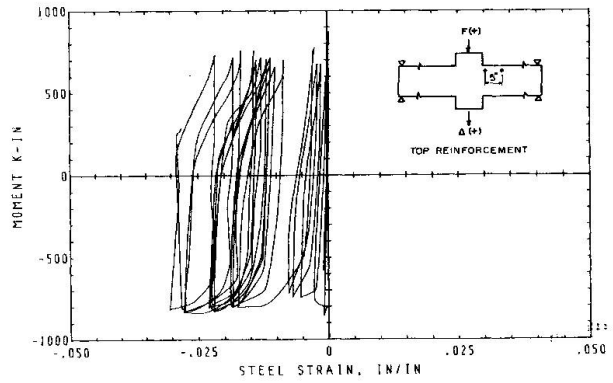


Fig. 8 Steel Strain History (Beam 9)

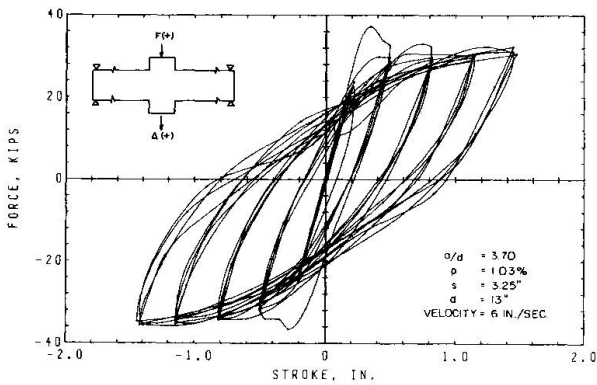


Fig. 5 Inelastic  $F - \Delta$  Hysteresis Loops (Beam 9)

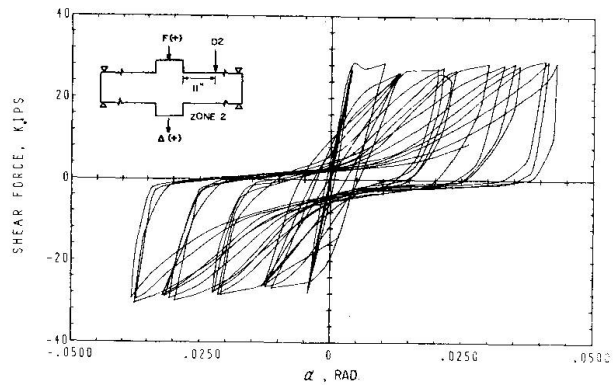


Fig. 9 Shear Deformation Index (Beam 12)



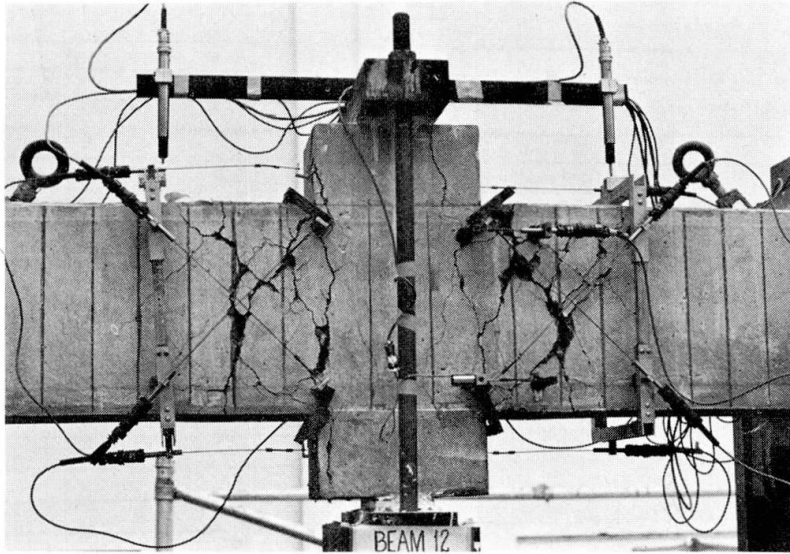


Fig. 10: Beam 12 After Test

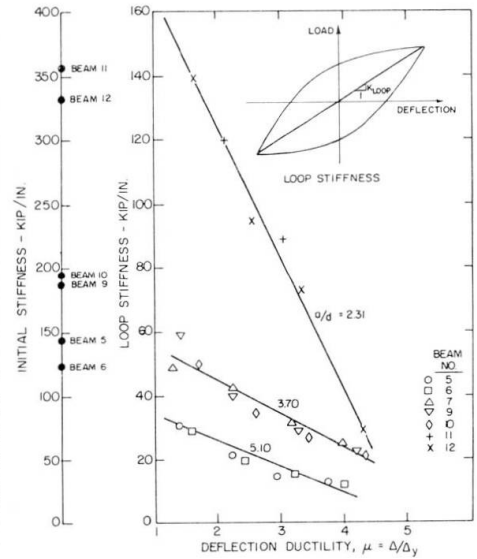


Fig. 11: Loop Stiffness Degradation

ANALYSIS OF TEST RESULTS

As observed in Fig. 3, deflection cycling within the elastic limit results in hysteresis loops which decrease in area by as much as 50% even when the cycling is repeated at a constant amplitude of deflection.

Except for increases in yield strengths by as much as 20%, no significant differences existed in the hysteresis loops of similar beams tested under dynamic and quasi-static conditions. The increase in yield strength influences energy absorption only for the cycle during which yielding takes place.

An important characteristic of reinforced concrete beams is the continuous deterioration of stiffness with increasing amplitudes of deflection or ductility. The deterioration of the instantaneous stiffness is exhibited by the hysteresis loops. Shear pinching can significantly influence instantaneous stiffness. Therefore, in such cases the elasto-plastic Ramberg-Osgood, or Clough's degrading stiffness models (9) are not applicable.

A more refined "loop stiffness" can be defined as the ratio of the sum of the maximum loads to the sum of the maximum displacements. This stiffness is especially appropriate for the beams tested since equal top and bottom reinforcements have been used and symmetrical displacements have been applied. A summary of the loop stiffness versus deflection ductility is seen in Fig. 11. As observed, loop stiffness deterioration is more significant for beams with smaller a/d ratios.

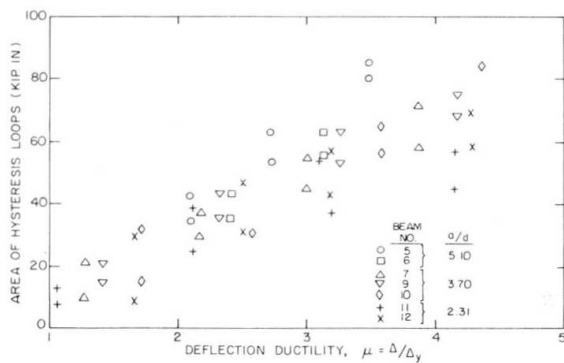


Fig. 12: Energy Absorption

Energy absorption is one of the most important properties directly linked to damping constants used in dynamic analyses. Using well defined cyclic loadings, energy absorption capacities were carefully measured in this investigation. Areas of the hysteresis loops obtained are summarized in Fig. 12. Except for increasing energy absorption with increasing ductility, no significant trend can be observed.

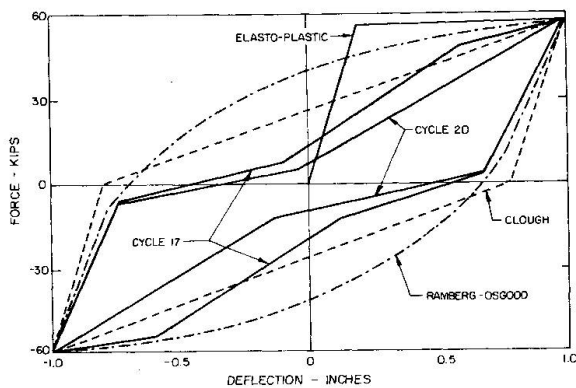


Fig. 13: Effect of  
Shear Pinching

When cycled at the same amplitude, energy absorption has significantly decreased after four cycles. Individually, however, shear pinching in each beam can be very important. For example, in fig. 13, the areas of hysteresis loops 17 and 20 of beam No. 12 are 65% and 54.5% respectively, of the area of the loop described in Clough's degrading stiffness model. Thus, it can be seen that shear pinching can significantly reduce energy absorption capacity.

While recent codes (7,8) recommend the use of #3 stirrups at  $d/4$  spacing, it is observed for the beams tested that no significant differences of energy absorption or stiffness deterioration exist between beams with stirrup spacing of 3.25" ( $d/4$ ) or 6". Therefore, the  $d/4$  spacing requirement should be relaxed for beams with normal range of nominal shear stresses.

#### CONCLUSIONS

The only observed influence of dynamic loading is an increase in yield strength. No other strain rate effects are observed. Energy is dissipated within and beyond the elastic limit. The areas of hysteresis loops decrease continuously when cycled under load reversals at the same amplitude. The energy absorption increases with an increase in ductility. Stiffness deterioration is more significant in shear span with smaller  $a/d$  ratios. Shear pinching in shear spans must be represented in mathematical models in order to correctly characterize their seismic behavior. For low nominal shear stresses it appears that the  $d/4$  spacing requirement for web reinforcement in critical regions should be relaxed.

#### REFERENCES

1. Brown, R.H., and Jirsa, J.O., "Reinforced Concrete Beams Under Load Reversals," Journal of ACI, May 1971.
2. Bertero, V.V., Bresler, B., and Liao, H., "Stiffness Degradation of Reinforced Concrete Members Subjected to Cyclic Flexural Moments," EERC Report 69-12, University of California, Berkeley, Dec. 1969.
3. Burns, N.H., and Siess, C.P., "Repeated and Reversed Loading in Reinforced Concrete," PROC., ASCE, Vol. 92, ST5, Oct. 1966.
4. Hanson, N.W., and Conner, H.W., "Reinforced Concrete Beam-Column Connection for Earthquakes," Preliminary Report, PCA, Nov. 1965.
5. \_\_\_\_\_, "Experimental Studies on Load-Deflection Characteristics of Reinforced Concrete Columns Subjected to Alternate Loading," Report of the Training Institute for Engineering Teachers, Yokohama National Univ., March 1968.
6. Umemura, H., Aoyama, H., and Ito, ., "Experimental Studies on Reinforced Concrete Members and Composite Steel and Reinforced Concrete Members," University of Tokyo, Dec. 1970.

7. \_\_\_\_\_, "Building Code Requirements for Reinforced Concrete," (ACI-318-71), American Concrete Institute, 1971.
8. \_\_\_\_\_, Uniform Building Code, 1970 ed.
9. Clough, R.W., "Effect of Stiffness Degradation on Earthquake Ductility Requirements," Structural Eng. Lab. Report No. 66-16, U.C. Berkeley, Oct. 1966.
10. Bertero, V.V., et.al., "Rate of Loading Effects on Uncracked and Repaired Reinforced Concrete Members," EERC Report 72-9 (to be published).

## SUMMARY

The behavior of reinforced concrete components simulating interior beams and column stubs is investigated. Stirrup spacing, shear span to depth ratio and loading velocity were varied in order to study their influences on energy absorption and stiffness degrading properties of beams so all beams were loaded by hydraulically powered, electronically controlled actuator. Load-deflection and other pertinent relationships are discussed in terms of energy absorption, stiffness deterioration, strength and deflection ductility.

## RESUME

On étudie le comportement d'éléments en béton armé simulant des poutres intérieures et des tronçons de colonne. L'espacement des étriers, le rapport de la portée de cisaillement à la hauteur et la vitesse de charge ont été variés pour étudier leurs influences sur l'absorption d'énergie et sur la perte de rigidité des poutres. Toutes les poutres ont été chargées par un servomoteur actionné hydrauliquement et contrôlé électroniquement. On discute ensuite les courbes charge-déformation ainsi que d'autres relations intéressantes en termes d'absorption d'énergie, de perte de rigidité, de résistance et de déformabilité.

## ZUSAMMENFASSUNG

Man untersucht das Verhalten von Stahlbetonteilen, welche Balken und kurze Säulenstücke darstellen. Die Bügelanordnung, das Verhältnis von Spannweite zur Höhe und die Belastungsgeschwindigkeit wurden variiert, um ihre Einflüsse auf die Energieabsorption und steifigkeitsreduzierenden Eigenschaften der Balken zu studieren; alle Balken wurden hydraulisch beladen und elektronisch überwacht. Die Lastverformungsabhängigkeit und andere signifikante Verhältnisse werden in Form von Energieabsorption, Steifigkeitsabnahme, Widerstand und Verformungsduktilität besprochen.

## Elasto-Plastic Cyclic Horizontal Sway Behaviours of Reinforced Concrete Unit Rigid Frames subjected to Constant Vertical Loads

Comportements élasto-plastiques de cadres en éléments de béton armé soumis à des charges verticales constantes lors de mouvements cycliques horizontaux

Elastoplastisches zyklisches horizontales Schwingungsverhalten von Stahlbetonrahmen unter konstanter vertikaler Belastung

Minoru YAMADA  
Professor Dr.-Ing.

Hiroshi KAWAMURA  
Wiss. Ass. Dipl.-Ing.

Kazuo KONDOH  
Dipl.-Ing.

Department of Architecture, Faculty of Engineering  
Kobe University  
Kobe, Japan

### 1. INTRODUCTION

To make clear the fundamental cyclic deformation behaviors of reinforced concrete rigid frames, various constant deflection amplitude tests are carried out on reinforced concrete unit rectangular rigid frames subjected to constant vertical loads. "The Critical Strain-Point Method"<sup>(1)</sup> with the idealized cross section and the idealized material properties are applied for analysis. The computed values are compared with tested results.

### 2. TESTS

#### 2-1. Test Specimens

The test specimens of reinforced concrete unit rectangular rigid frames are shown in Fig.1 (a) and (b). The length of span and height of the frames are 120cm, 60cm, respectively, and the cross section of the columns and beams are 12.5cm x 12.5cm, with reinforcement ratios of:

Series (a)  $p_{Beam}=1.6\%$ ,  $p_{Column}=0.3\%$ ;

Series (b)  $p_{Beam}=0.9\%$ ,  $p_{Column}=0.9\%$ .

The mix proportion of the concrete is 1:2.55:3.34 with a water-cement ratio of 60% by weight with high quality portland cement and river gravel aggregate. The mechanical properties of concrete and reinforcing steels are indicated in Tables 1 and 2.

#### 2-2. Loading and Measureing System

The test specimens are loaded in such a mechanism as shown in Fig.2. The cyclic lateral forces  $P$  are loaded by oil jacks with load cells through diagonal high tensile strength bars, and constant vertical load  $N$  is loaded by testing machine through needle roller bearings with a friction coefficient of 1/1000. The lateral sway displacement of frames are measured by dial gages fixed upon the measureing frames which are set upon the test piece at the center of the corner through knife edges and supported by roller at the opposite corner.

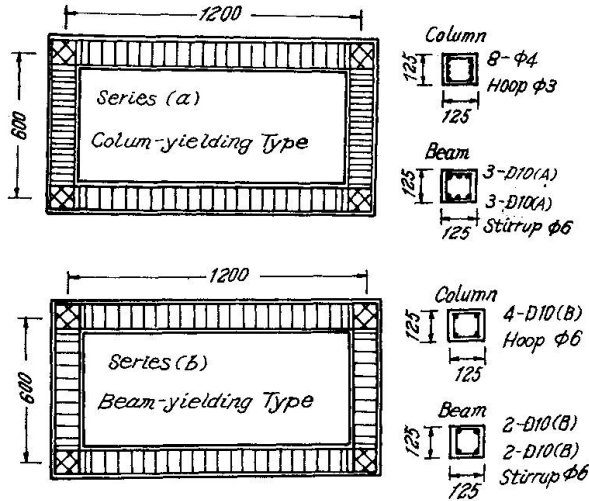


Fig.1 Test Specimen

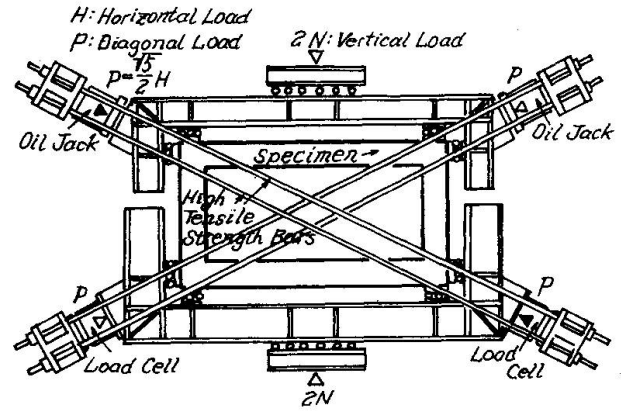


Fig.2 Loading System

2-3. Test Results

Tests are carried out on both series (a) and (b) in order to make clear the effects of constant vertical load levels and the effects of displacement amplitudes upon the deformation and fracture behaviors.

The constant vertical load level, it is selected here  $1/3N_0$  and  $1/6N_0$ , where  $N_0$  is the ultimate strength of centrally loaded column, and as displacement amplitudes  $\pm 0.100h$ ,  $\pm 0.050h$ ,  $\pm 0.033h$ ,  $\pm 0.025h$ , where  $h$  is story height.

Test results are shown in Fig.3, the lateral sway displacement  $\delta$  (in mm) or relative story displacement angle  $R(\delta/h)$  in abscissa and the lateral load  $H(= \frac{2}{15}P, P$ :diagonal load) in ordinate.

The mark X represents the point at which the vertical resistance, i.e. the constant vertical load of column, become unable to sustain the definite constant value, namely, the collapse of frames (Figs.3 (a)-1,2,5; (b)-1,4).

CTC, CCC indicate the formation of the tensile cracks and compressive cracks at column's surface, BTC, BCC the tensile cracks and compressive cracks at beam's surface and PSC the shear cracks at the frame corner, respectively.

The deformation characteristics, cracking patterns and the fracture modes are distinguished into two types;

Series (a) the column-yielding type,  
Series (b) the beam-yielding type.

Table 1 Mechanical Property of Concrete

Specimens	$c\sigma_c$ (% $\text{cm}^2$ )	$c\sigma_c$ (% $\text{cm}^2$ )	Series
RCR:B16C03:1/3 $N_0$ :Ra= $\pm 0.100$	340	25.8	Series (a) Column- yielding Type
RCR:B16C03:1/3 $N_0$ :Ra= $\pm 0.050$	323	25.6	
RCR:B16C03:1/3 $N_0$ :Ra= $\pm 0.025$	363	31.8	
RCR:B16C03:1/6 $N_0$ :Ra= $\pm 0.100$	321	26.0	
RCR:B16C03:1/6 $N_0$ :Ra= $\pm 0.050$	341	29.1	
RCR:B16C03:1/6 $N_0$ :Ra= $\pm 0.025$	329	25.0	
RCR:B1C1 : 1/3 $N_0$ :Ra= $\pm 0.100$	331	26.3	Series (b) Beam- yielding Type
RCR:B1C1 : 1/3 $N_0$ :Ra= $\pm 0.033$	317	29.9	
RCR:B1C1 : 1/6 $N_0$ :Ra= $\pm 0.100$	320	28.9	
RCR:B1C1 : 1/6 $N_0$ :Ra= $\pm 0.033$	338	30.2	

Table 2 Mechanical Property of Steel

Reinforcing Bar	$s\sigma_s$ (% $\text{cm}^2$ )	$s\sigma_{max}$ (% $\text{cm}^2$ )
D-10 (A)	3900	5920
D-10 (B)	3730	5370
$\phi$ -6	2350	3250
$\phi$ -4	3700	4810
$\phi$ -3	3110	4420

D: Deformed Bar  $\phi$ : Round Bar

3. ANALYSIS

3-1. Assumptions

For the deformation analysis the "Critical Strain-Point Method"<sup>1)</sup>, which was introduced by the authors, is applied. The reinforced concrete cross section is idealized into 3-Point-Model (Fig.4). The Stress-Strain relationships of concrete and reinforcement are idealized into poly-linear models (Fig.5 (a),(b)).

3-2. Bending Moment-Curvature Relationships

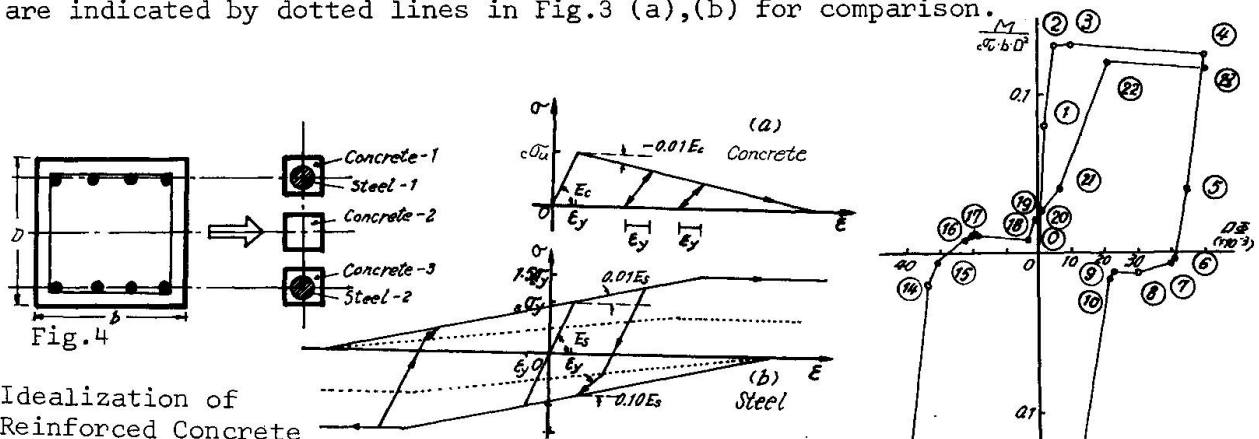
Bending moment-curvature relationships of reinforced concrete cross section is deduced from the critical strain point such as shown in Fig.6. As an example series (a) column-yielding type, RCR:B16C03:1/3No:Ra=0.050, is shown.

3-3. Load-Displacement Relationships

From the moment-curvature relationships (Fig.6), the load-displacement relationships are able to be computed as a total deformation of the rotation increments of plastic hinged region and elastic deformation of other parts such as shown in Fig.7. Fig.8 shows the strain states in a cross section at column ends (hinged part). The numerals in circles in Figs.6,7 and 8 correspond to each other. The stress states in 3 parts in the cross section expressed by critical strain point in Fig.7 are indicated in Fig.8 with corresponding numerals. From these figures, the stress states in arbitrary deformation states are clearly shown.

3-4. Computed Results

The computed results by the above mentioned critical strain-point method are indicated by dotted lines in Fig.3 (a),(b) for comparison.



Idealization of Reinforced Concrete Cross Section

Fig.5 Stress-Strain Relationships

Fig.6 M-φ Relationships

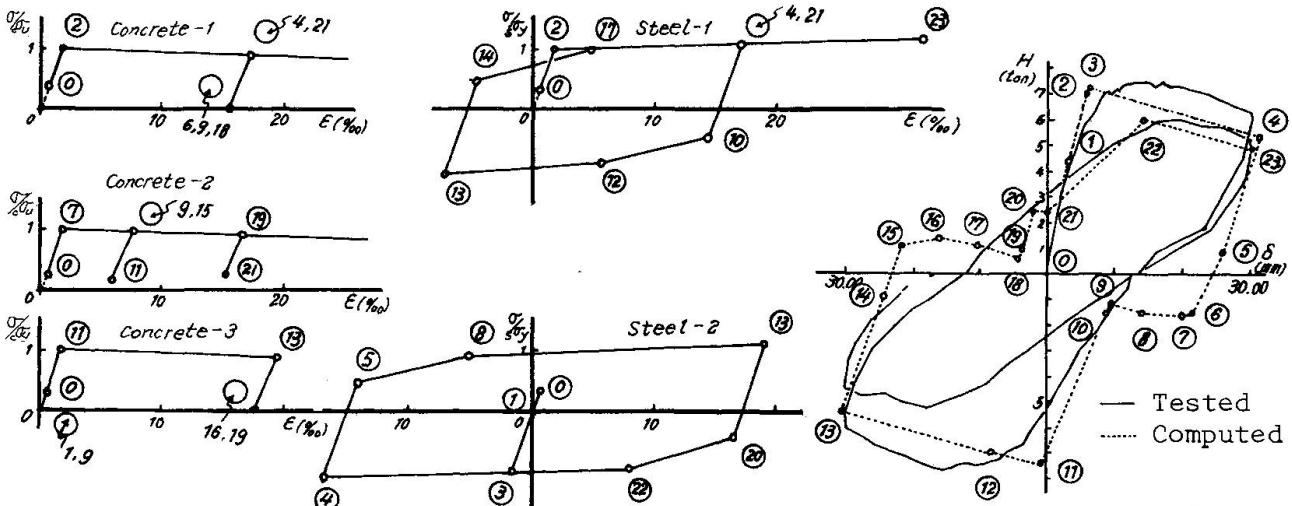


Fig.8 Process of Stress-Strain Relationships

Fig.7 H-δ Relationships



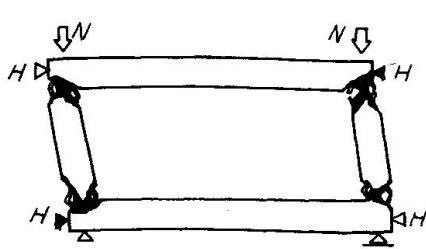
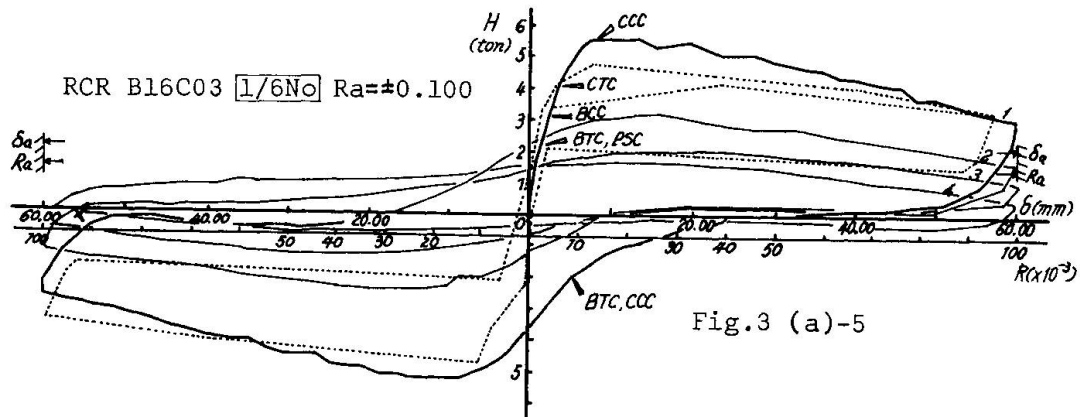
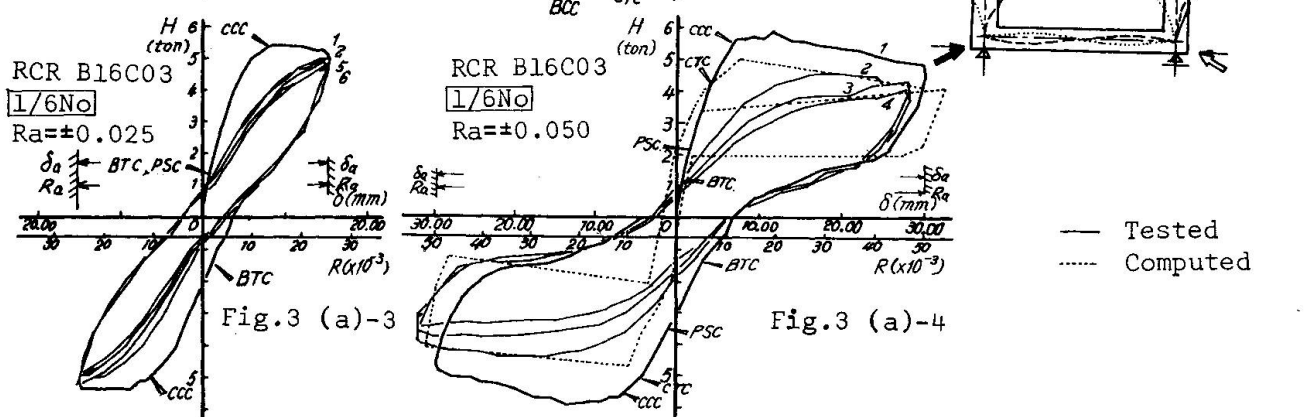
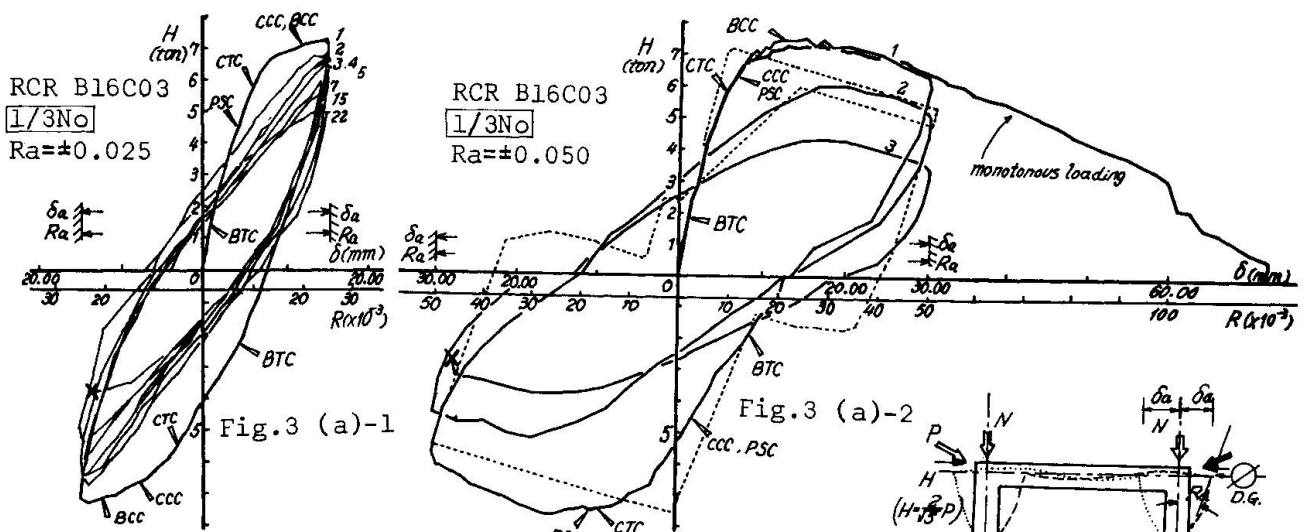


Fig.3 (a)-5\*\* Final State

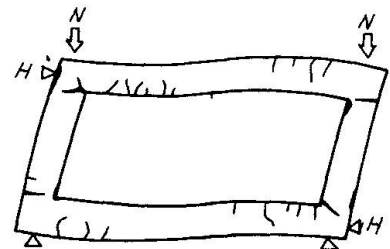


Fig.3 (a)-5\* Cracking Patterns at the End of Virgin Cycle

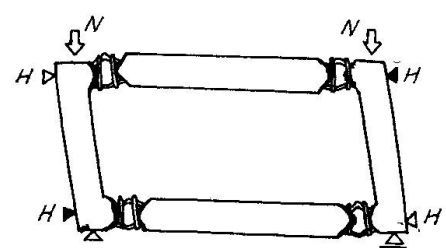
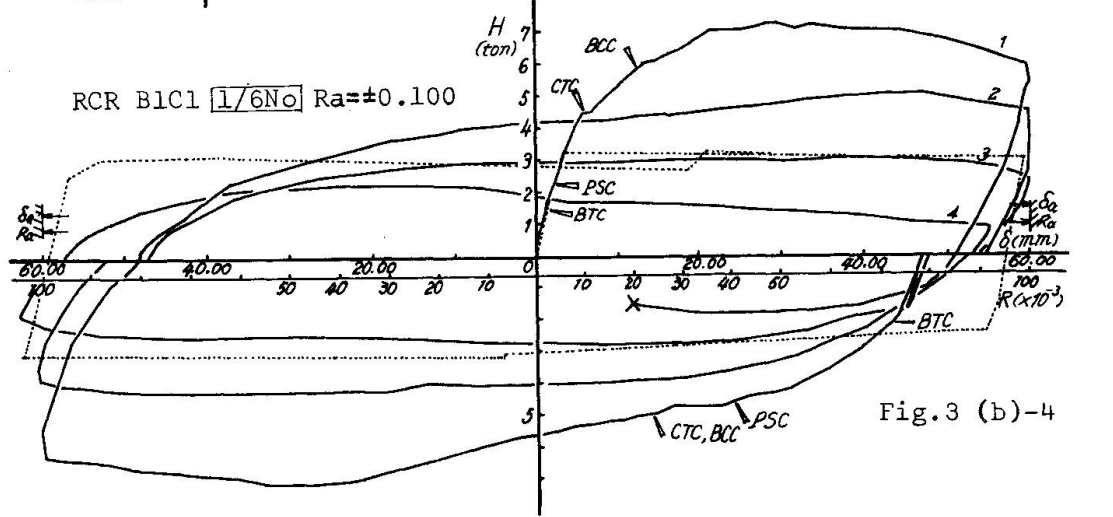
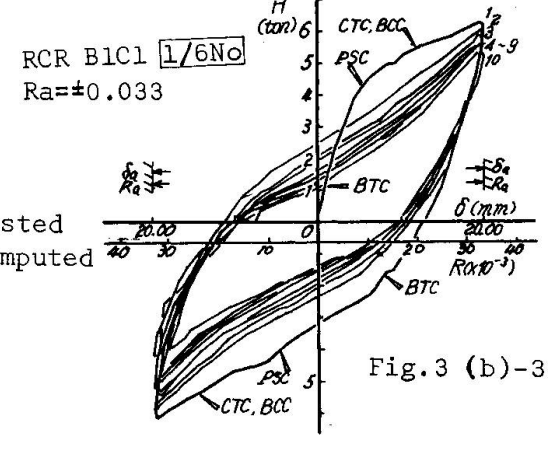
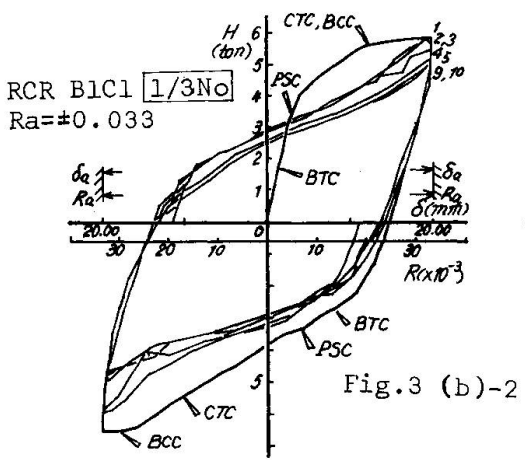
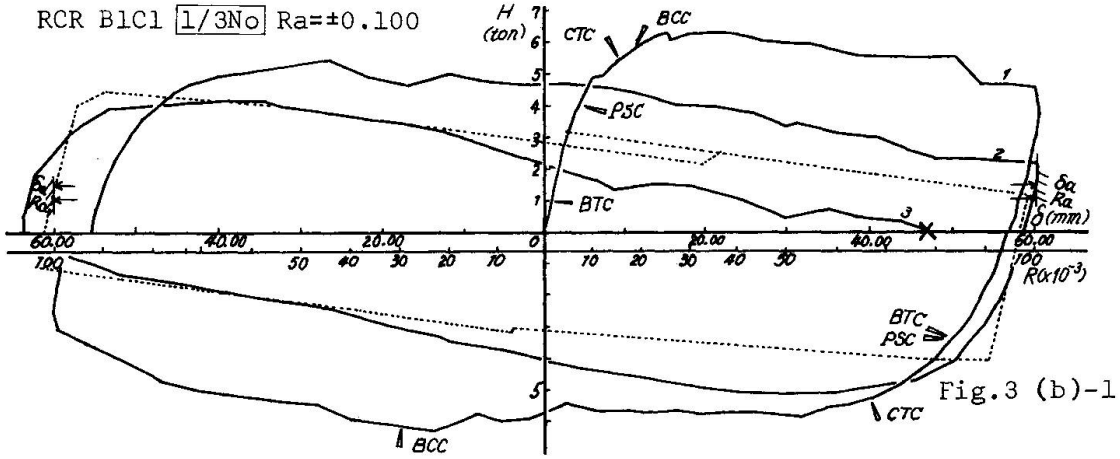


Fig. 3 (b)-4\*\* Final State

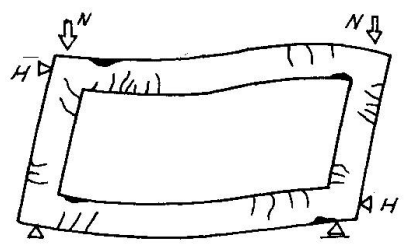


Fig. 3 (b)-4\* Cracking Patterns at the End of Virgin Cycle



#### 4. DISCUSSIONS AND CONCLUDING REMARKS

In the case of the column-yielding type (a) under the constant vertical load level of  $1/3N_0$ , H- $\delta$  loops show softening type and resisting capacity (H) deteriorates with the increase of the number of cycles, caused by the fatigue at the ends of columns, Figs.3 (a)-1,2.

Under the vertical load level of  $1/6N_0$ , with smaller displacement amplitude such as  $0.025h$ , H- $\delta$  loops show softening type and become steady state after several cycles (Figs.3 (a)-3). However, with larger amplitudes,  $0.050h$  and  $0.100h$ , H- $\delta$  loops show slipping type, and resisting capacity (H) deteriorates with the increase of the number of cycles, caused by the fatigue at the ends of columns (Figs.3 (a)-4,5).

On the other hand, in the case of the beam-yielding type (b) with larger amplitude such as  $0.100h$ , H- $\delta$  loops show softening type, and resisting capacity (H) deteriorates with the increase of the number of cycles, caused by the fatigue at the ends of beams (Figs.3 (b)-1,4). With smaller displacement amplitude such as  $0.033h$ , H- $\delta$  loops show hardening type, and become steady state after several cycles (Figs. 3 (b)-2,3). The differences of constant vertical load level ( $1/3N_0$ ,  $1/6N_0$ ) are not so remarkable in this type (b).

In this research, the fundamental elasto-plastic deformation characteristics of reinforced concrete unit rectangular rigid frames are made clear experimentally, and the physical meanings of the load-displacement hysteresis loops are well explained by the analysis, too.

#### 5. REFERENCES

1) . Yamada, M., Kawamura, H. :Elasto-plastische Biegeformänderungen der Stahlbetonsäulen und -balken(einseitige Biegung unter Axiallast), Abh., IVBH, Bd. 28/1, 1968, Zürich, S.193/220.

#### SUMMARY

Constant sway displacement amplitude tests on reinforced concrete unit rectangular rigid frames are carried out. The effects of vertical load level and displacement amplitudes upon the hysteresis loop characteristics are clarified on two series ((a) column-yielding type and (b) beam-yielding type) (Figs. 3 (a), (b)). Analytical values computed by the "Critical Strain-Point Method" are compared with test results. The coincidence between them are reasonable.

#### RESUME

On présente des essais effectués sur des cadres en éléments de béton armé soumis à des mouvements cycliques horizontaux. Les influences de l'intensité de la charge verticale et de l'amplitude des déplacements sur les caractéristiques de la boucle d'hystérésis sont classées en deux groupes: a) type colonne en domaine d'écrouissage, b) type poutre en domaine d'écrouissage, (Fig. 3 (a), (b)). Les valeurs analytiques obtenues par la méthode du point de déformation critique sont comparées aux résultats des essais. La coïncidence avec ces derniers est acceptable.

#### ZUSAMMENFASSUNG

Es werden Versuche mit konstanter Schwingungsamplitude an Einheits-Stahlbetonrahmen ausgeführt. Die Wirkungen der vertikalen Last- und Verformungsgrößen auf die Hysteresis-Schleife werden in zwei Serien geklärt: a) Typ des Stützen-Versagens und b) Typ des Balken-Versagens, (Fig. 3 (a), (b)). Nach der "Critical Strain-Point Method" gerechnete Werte werden mit Versuchsergebnissen verglichen. Die Übereinstimmung der Werte ist vernünftig.

### Behaviour of Multi-Storey Reinforced Concrete Frames subjected to Severe Reversing Loads

Comportement de cadres à plusieurs étages en béton armé soumis à des charges alternées importantes

Verhalten mehrstöckiger Stahlbetonrahmen unter starker Wechselbelastung

Richard N. WHITE  
Professor  
Dept. of Structural Engineering  
Cornell University  
Ithaca, N.Y., USA

Asadul H. CHOWDHURY  
Graduate Research Assistant  
Dept. of Agricultural Engineering  
Cornell University  
Ithaca, N.Y., USA

There have been numerous experimental studies undertaken on reinforced concrete beams and other elements subjected to reversing loads. In recent years increasing attention has been given to more complex structural geometries under the same type of loadings, such as member-joint assemblages and portal frames. The present discussion proceeds one step further in that it treats the behavior of three-story, two-bay reinforced concrete frames subjected to a fixed level of gravity load and reversing lateral loads that simulate earthquake forces.

The study has been conducted utilizing small scale models. The difficulties and expense of loading large multistory frames made the model approach the only feasible way to study the problem within a limited budget of a normal research project. Although models have been highly successful in a number of research projects at Cornell University on the inelastic performance of reinforced concrete structures, it was felt necessary to further substantiate their ability to portray all levels of the complex behavior encountered in multi-story frames under reversing loads. Therefore, a preliminary study was undertaken to compare the results of seven 1/10 scale models with full-scale prototype tests for beam-column joints of a building (Fig. 1 shows the model dimensions). The prototypes (Ref. 1) represented the exterior beam-column joint of a high rise building

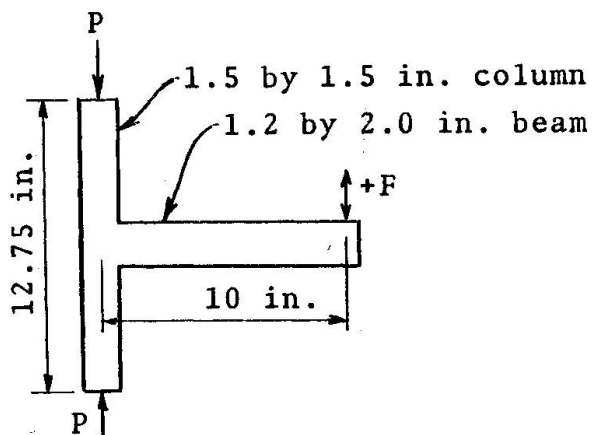


Fig. 1 - Beam-column model specimen geometry

between column inflection points and the beam inflection point. The prototypes and models were loaded with reversing bending of the beam according to the following schedule:

Cycle:	1	2	3	4	5
D.F. :	3/4	2.5	4	3/4	3/4

Cycle:	6	7	8	9
D.F. :	3/4	5	5	5

where D.F. is the ductility factor, defined as the ratio of the total rotation at a length of one-half the beam depth from the critical section at maximum applied

load to that at yield load. The column of each specimen was also subjected to simultaneous axial load.

The key to successful modeling of inelastic behavior of reinforced concrete structures is in meeting similitude requirements for model materials. Extensive development work was needed to obtain microconcretes with proper compressive and tensile strengths and stress-strain characteristics, and deformed model reinforcement with proper yield point and work hardening properties. Details on materials, as well as full reporting of model results, are given in Ref. 2.

Selected results are given in Figs. 2 and 3. Fig. 2 gives prototype and scaled model moment-rotation response for prototype specimen I-A for cycles 1, 2, 3, and 7. A comparison of major

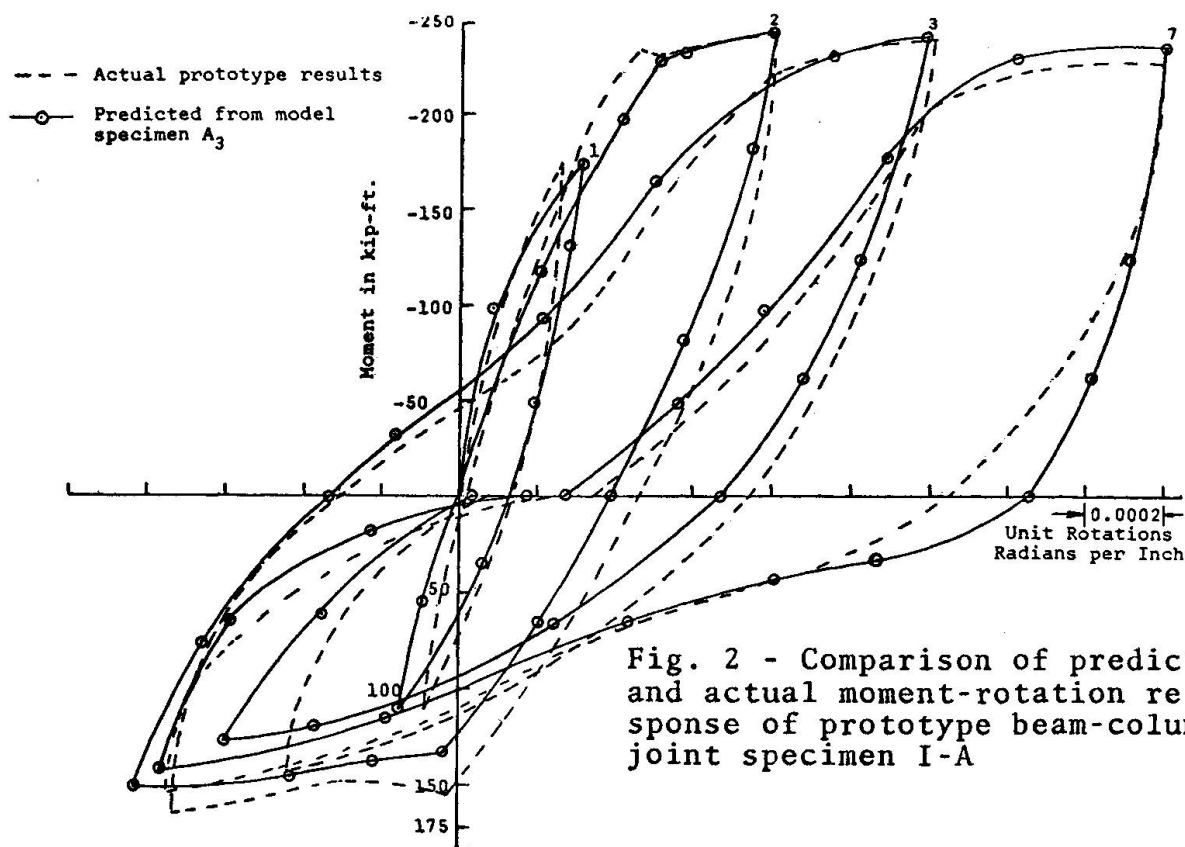


Fig. 2 - Comparison of predicted and actual moment-rotation response of prototype beam-column joint specimen I-A

cracking patterns for the same specimen is shown in Fig. 3; a remarkably similar pattern of cracking is evident in model and prototype. Model and prototype beam deflection correlations were equally good. These correlations are considered to be excellent in that identical prototype specimens would not be expected to compare any more favorably. Model predictions for beam and column reinforcing steel stresses and for other prototype specimen designs were also good to excellent. Diagonal cracking in the columns of some models was not modeled properly; in each case the model concrete compressive strength was some 15-20% higher than that of the prototype specimen. It is absolutely essential that the model material similitude requirements be met as closely as

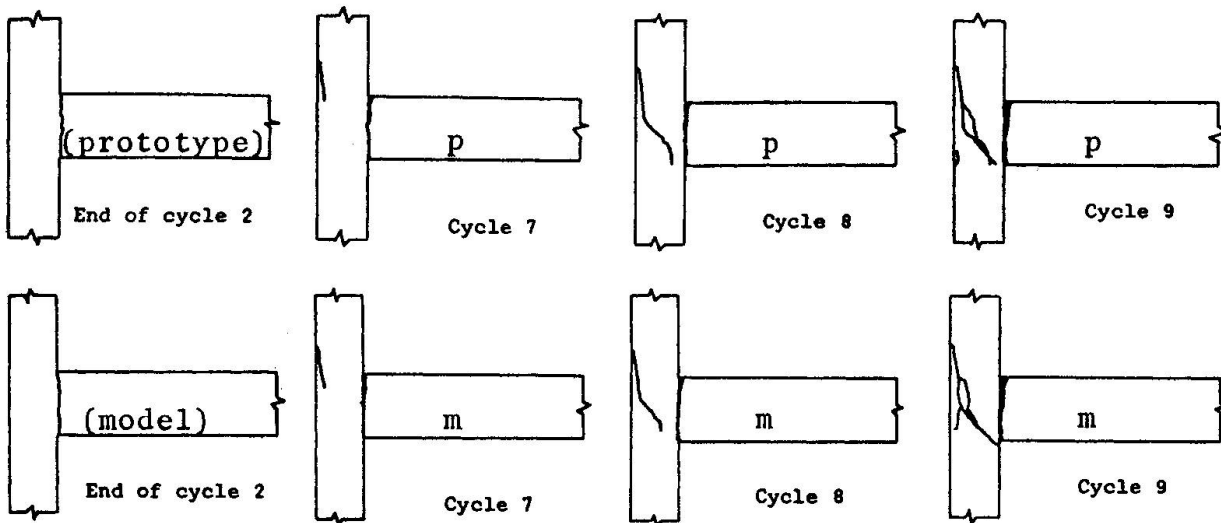


Fig. 3 - Crack patterns for Prototype I-A and model A3 at peak downward loadings (major cracks only)

possible for small scale modeling of complex inelastic reversing load effects.

The second part of this paper treats the behavior of 1/10 scale, three-story, two-bay reinforced concrete model frames subjected to combined gravity and lateral loads. One frame was loaded with 1.4 specified gravity load and a monotonically increasing lateral load up to failure. The second frame has the same gravity load and cyclic, reversing lateral loads of varying intensity. Defining the lateral load factor (LLF) as the ratio of applied lateral load to the design lateral load, the loading history is summarized on the next page. The model frame dimensions are given in Fig. 4.

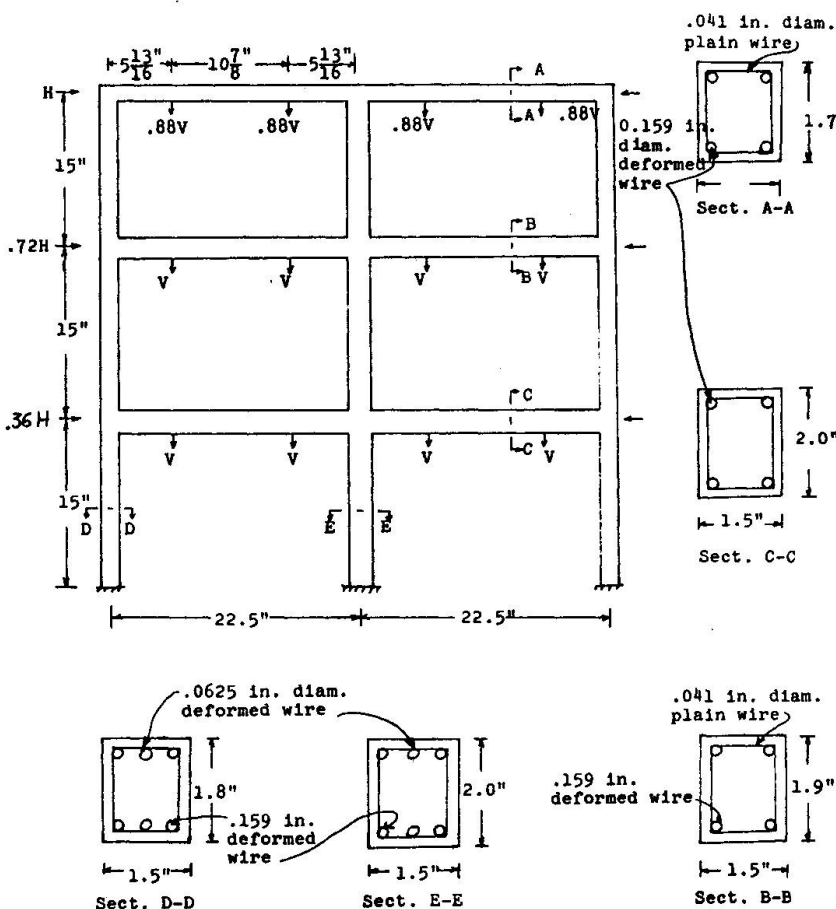


Fig. 4 - Frame details

Cycle:	1	2	3	4	5	6	7	8	9
LLF:	1	3	3	3	3	5	5	5.5	6

The frames were designed to conform in all details to the requirements of the Structural Engineers Association of California Recommendations for Seismic Design. Selected results presented here include comparisons between the monotonically loaded and cyclically loaded frame, and comparisons with theory.

Details of the entire study, including the modeling techniques employed, are given in References 2, 3, and 4. Gravity loads were applied with gravity load simulators that allowed free translation of the frame. Lateral loads were applied with mechanical jacks that permitted rather precise control of the loading, even in the later cycles when behavior was highly inelastic.

The final cracking pattern of the frame subjected to nine cycles of lateral loading with a maximum lateral load factor of 6 is shown in Fig. 5 below. Each of the six beams in the frame has four crack forming regions (two positive and two negative moments). Fig. 5a shows the final cracking pattern of the bottom story interior beam-column joint. At the peak of the first cycle, with LLF = 1, no flexural cracking was visible in the joint. For the first half of the second cycle (LLF = 3), when the lateral loads were applied from the left side of the frame, the top of the left beam yielded and a wide flexural crack was visible. On unloading, the crack narrowed but remained visible. In the second half of this cycle, cracks appeared in the right beam due to the yielding of the top bars, and the cracks in the left beam widened. At the completion of cycle 2, with LLF = 0, the cracks in both beams closed partially but remained visible.



Fig. 5 - Cyclically loaded frame

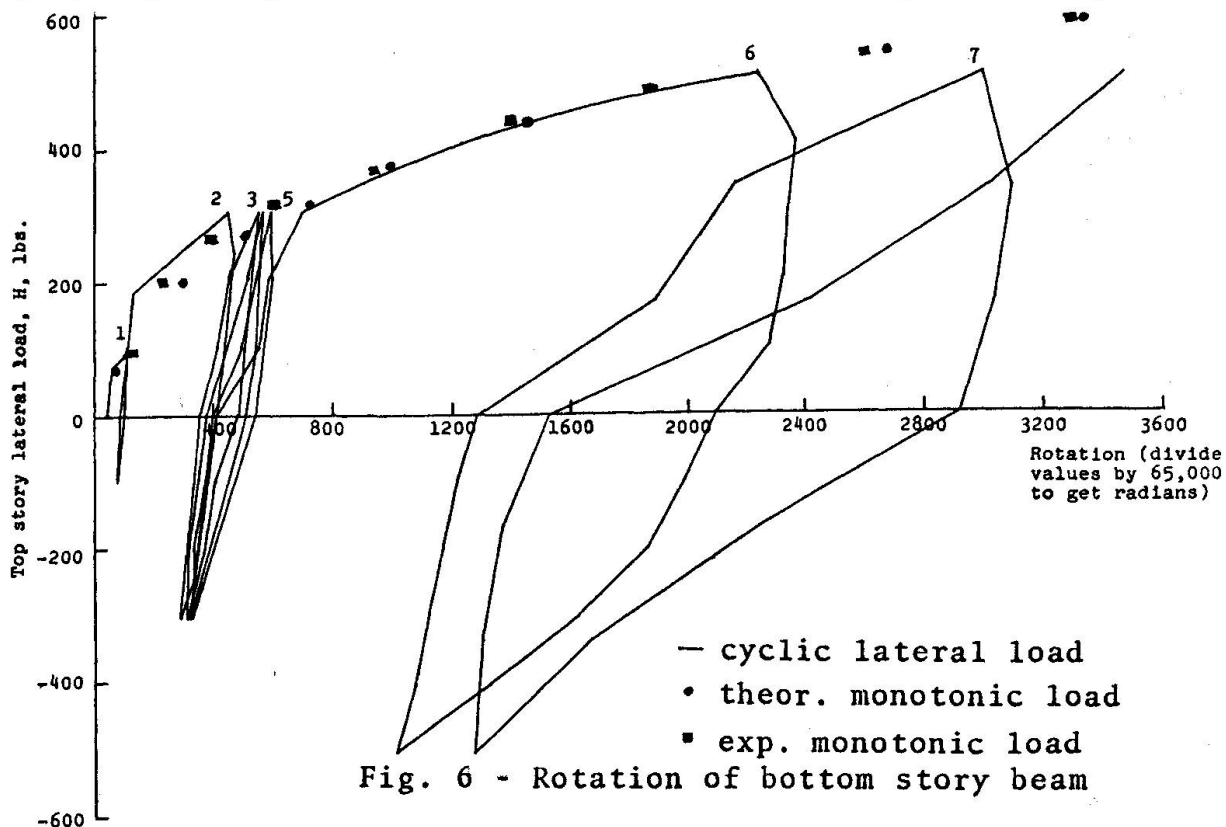


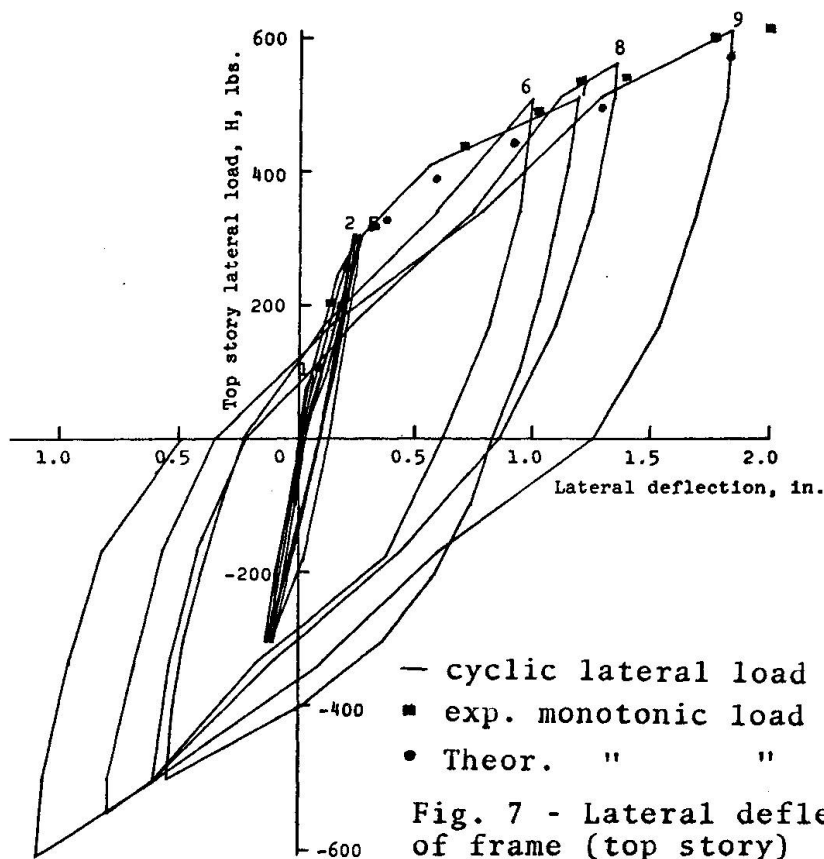
The sequence of crack formation and crack widening in other critical sections of the frame was similar to that described above. It is recognized that fewer cracks are visible in the model than in the prototype, but extensive modeling studies have shown that this does not produce any measurable differences in the moment-rotation and load-deflection characteristics of the model structure.

First visible cracking at the bases of the columns was observed at the sixth cycle (LLF = 5). Column crack widths increased substantially in subsequent cycles.

The application of cyclic loads produces alternating diagonal tension forces in the joint regions of the frame. These forces may produce deterioration of reinforcement anchorage, yielding of shear reinforcement, additional yielding of beam steel, and shear failure of the joint itself. In order to prevent these inelastic deformations of the joint area, and to avoid shear failure and other non-ductile behavior, proper reinforcement detailing must be followed in the joint areas and other regions with high shear and anchorage forces. As shown in Fig. 5, no cracks appeared in any joints in the frame designed and detailed according to earthquake resistant design specifications which give major emphasis to the details of transverse reinforcement and anchorage lengths in the joint regions.

Fig. 6 shows the top story lateral load vs. the rotation of the bottom story beam. A comparison between the curves for the cyclically load and unidirectionally loaded frames shows that properly designed frames do not deteriorate significantly under





severe cyclic loads. The load-deflection characteristics of the two frames (Fig. 7) also supports this conclusion. The indispensable role of compression reinforcement and closely spaced ties in providing toughness and ductility is apparent from these tests.

**Acknowledgment:** Partial support for this study was provided by the National Science Foundation (Grant GK-13992).

#### References:

1. Hanson, N.W. and Conner, H.W., "Seismic Resistance of Reinforced Concrete Beam-Column Joints," *Journal of the Structural Division, ASCE*, Vol. 93, October 1967, p. 533.
2. Chowdhury, A.H., "Inelastic Behavior of Small Scale Reinforced Concrete Beam-Column Joints Under Severe Reversing Loads," Department of Structural Engineering Report #342, Cornell University, October 1971.
3. Chowdhury, A.H., White, R.N., and Scott, N.R., "Multi-Story Reinforced Concrete Frame Models," Meeting Preprint 2002, ASCE National Structural Engineering Meeting, San Francisco, California, April 1973.
4. Chowdhury, A.H., "An Experimental and Theoretical Investigation of the Behavior of Reinforced Concrete Multi-Story, Multi-bay Frame Models Subjected to Simulated Seismic Loads," A Ph.D. thesis to be submitted to the Graduate School of Cornell University, Ithaca, New York, September, 1973.

#### SUMMARY

Small scale models are shown to be an excellent approach for investigation of reversing load phenomena in reinforced concrete. Three-story, two-bay frames were tested under simulated seismic loads and reached lateral force levels of 6 times the design values for both unidirectional and cyclic lateral loadings. Properly designed frames (closely spaced ties, compressive reinforcement, and adequate anchorage lengths) do not deteriorate significantly under severe cyclic lateral loadings.

## RESUME

Les modèles à petite échelle s'avèrent très intéressants pour l'étude du phénomène des charges alternées dans les structures en béton armé. Des portiques multiples à trois étages et doubles travées soumis à des charges sismiques simulées et à des forces latérales dont l'intensité atteint six fois la valeur de dimensionnement ont été testés à la fois pour des charges latérales uni-directionnelles et pour des charges cycliques. Les portiques correctement dimensionnés (armatures peu espacées, armatures de compression, longueurs d'encrage adéquates) ne sont pas particulièrement endommagés même soumis à des charges cycliques latérales importantes.

## ZUSAMMENFASSUNG

Es wird gezeigt, dass Modelle in kleinem Massstab eine sehr gute Annäherung an die Wirklichkeit für die Untersuchung von Lastumkehr-Phänomenen in Stahlbeton darstellen. Dreistöckige Rahmen mit 2 Oeffnungen wurden unter simulierter seismischer Belastung untersucht; die horizontale Kraft erreichte eine Grösse, die bis zu sechs mal den Bemessungswerten für gleichgerichtete und zyklische horizontale Belastung entspricht. Sauber bemessene Rahmen (engliegende Anker, Druckarmierung, genügende Verankerungslängen) verschlechtern sich nicht wesentlich unter starker horizontaler zyklischer Belastung.



Leere Seite  
Blank page  
Page vide

### Strength and Lateral Deformability of Columns of Reinforced Concrete at Shear Failure

Résistance et déformabilité latérale de colonnes en béton armé au stade de la rupture par cisaillement

Festigkeit und horizontale Verformbarkeit von Stahlbetonstützen bei Schubbruch

Kazuo OHNO  
Emeritus Professor

Takuji SHIBATA  
Professor  
Hokkaido University, Japan

Takashige HATTORI  
Assistant Professor

A number of reinforced concrete buildings suffered serious damages due to the 1968 Tokachioki earthquake in Japan. The injuries to columns were conspicuous in the damaged buildings and most of them resulted from shear failure. After the earthquake, experimental studies on the shear failure of reinforced concrete columns subjected to lateral forces have been carried out by many researchers in Japan. In the present paper, we propose equations to assess the shear strength and the ultimate lateral deformability at shear failure of reinforced concrete columns on the basis of the investigation of the test data which have been presented in Japan since 1961. The equation for the shear strength of columns is obtained through a modification of an empirical equation for the shear strength of beams, which has been proposed by K. Ohno and T. Arakawa and widely accepted in Japan because of its good applicability.

#### 1. Ohno-Arakawa's equation for shear strength of beams

In order to make shear failure precede flexural yield in a specimen subjected to the simple-beam type of loading, the specimen must be greatly over-reinforced with longitudinal reinforcement. Furthermore, the deformation of the portions of simple beams where shear cracks may occur is in single curvature, whereas the deformation of members in building frames subjected to lateral loads is generally in double curvature. For these reasons, it is open to question whether the test results on simple beams could be directly applied to the prediction on the behaviors of building frames. A special type of loading for shear test was proposed by K. Ohno, one

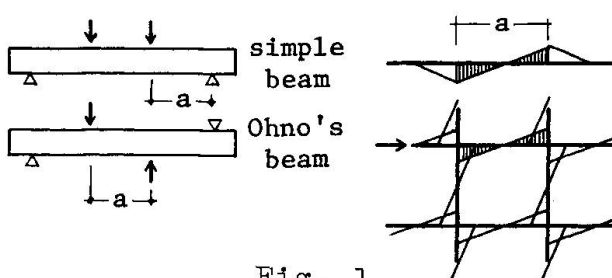


Fig. 1

of the authors, at the RILEM Symposium of 1957 in Stockholm. By use of this loading method, the actual conditions of stress and deformation of members in frames subjected to lateral loads can be reproduced in the testing specimens as shown in Fig. 1.

K. Ohno and T. Arakawa had performed the shear test on 156 beam-specimens with wide variations by adopting the Ohno's method and established the following empirical equation for the shear strength of reinforced concrete beams in building frames, in 1960.

$$\tau_u = \frac{V_u}{b_j} = k_u \cdot k_p \frac{0.23 (f'_c + 180)}{a/d + 0.23} + 2.7 \sqrt{p_w \cdot f_y} \quad (1)$$

where

$k_u$  = coefficient for size of specimen.

$k_p$  = coefficient for axial reinforcement ratio.

$a$  = shear span: distance between loading points.

$d$  = effective depth of beam.

$f'_c$  = compressive strength of concrete.

$p_w$  = web reinforcement ratio.

$f_y$  = yield point of web reinforcement.

This equation corresponds not only to the test results by the proposers but also to the test results on restrained beams performed by the groups at Illinois University: K.G. Moody, I.M. Viest, R.C. Elstner,

E. Hognestad in 1955 and

J.J. Rodriguez, A.C.

Bianchini, I.M. Viest,

C.E. Kesler in 1959,

with good concentration as shown in Fig. 3.

Recently, the authors

recommended an equation

for the shear strength of

simple beams, that

is Eq. (2), which is ap-

licable for only simple

beams with web re-

inforcement and suffi-

cient anchorage of

axial reinforcement at

the ends of the beams.

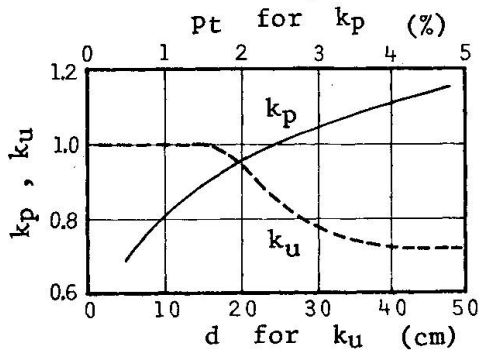


Fig. 2

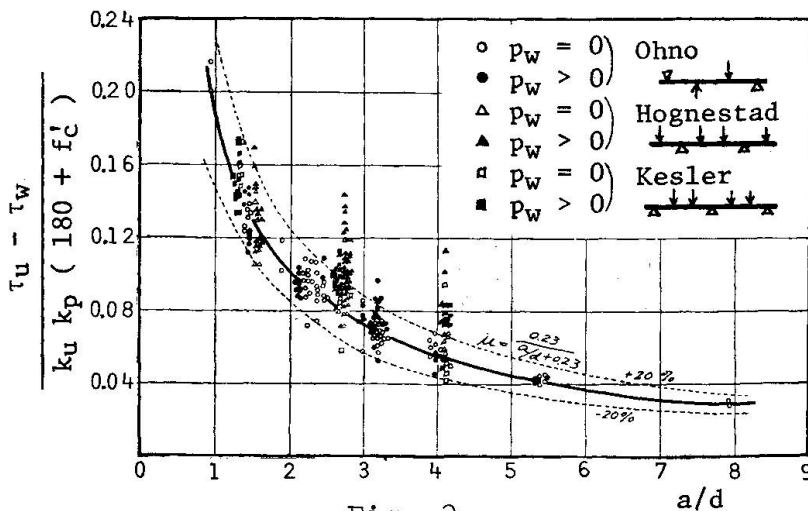


Fig. 3

$$\tau_u = \frac{V_u}{b_j} = k_u \cdot k_p \frac{0.23 (f'_c + 180)}{a/d + 0.23} + 1.4 \sqrt{p_w \cdot f_y} \quad (2)$$

where

$a$  = shear span: distance between loading point and support, cf. Fig. 1.

2. Outline of experimental works on shear resistance of reinforced concrete columns in Japan

Since 1961 in Japan, the shear tests of 378 column-specimens have been carried out by many researchers as shown in Table 1, where the data recognized as flexural failure by the investigator's own judgment are excluded. The types of loading in these investigations can be classified into three categories as follows:

- a) A specimen is laterally loaded by Ohno's method after introducing a certain magnitude of axial force in the specimen.
- b) A specimen is laterally loaded like a simple beam after introducing a certain magnitude of axial force in the specimen.
- c) A specimen of two-story-frame shape is laterally supported at the positions of the top beam and the bottom beam and laterally loaded at the position of the middle beam after introducing a certain magnitude of axial force in each of the columns.

The loading procedures and the number of specimens subjected to each procedure are shown in Table 2.

Table 1

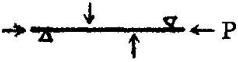

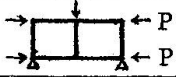
Type of loading	Investigator (Number of specimens)	Total
a) 	H.Aoyama(12), S.Bessho(9), T.Endo(3), M.Hirosawa(9), H.Muguruma(25), T.Nakayama(18), M.Wakabayashi(40), M.Yamada(37), authors(49)	9 (202)
b) 	T.Endo(7), A.Ikeda(104), T.Naka(12), T.Shimazu(5), T.Takeda(27) M.Yamada(1)	6 (156)
c) 	T.Takeda(2), authors(18)	2 (20)
Total		(378)

Table 2

Type of loading	Procedure of loading	Number of specimens		
		Total	For strength	For deforma.
a)	Monotonic increase	156	115	123
	Repeated reversal:			
	increase of peaks	25	9	8
	load limited	8	-	-
	deflection limited	13	-	-
b)	Monotonic increase	47	6	7
	Repeated reversal:			
	increase of peaks	68	27	27
	load limited	27	-	-
	deflection limited	14	-	-
c)	Monotonic increase	9	9	9
	Repeated reversal:			
	increase of peaks	11	9	11
Total		378	175	185

In the present paper, the data subject to one of the following conditions are excluded from the discussion with the intention of concentrating the investigation on the ultimate shear strength and the ultimate lateral deformability at shear failure: (1) the specimen subjected to repeated load by controlling with the load-limit lower than the ultimate shear strength or with the deflection-limit less than the deflection at the ultimate shear strength; (2) the data in which the value of a factor necessary to assess the ultimate shear strength is not shown; (3) the data in which there is no description about the deflection; (4) the specimen with a special type of web reinforcement, e.g. hoop of steel plate; (5) the specimen which ought to be considered to fail in flexure on the basis of the shape of load-deflection curve, the crack pattern and the comparison of the test result with the calculated result on the ultimate strength theory of flexure. Consequently the data available for the discussion on the ultimate shear strength are 175 specimens including 45 subjected to cyclic increasing loads and the data available for the discussion on the ultimate deformability at shear failure are 185 specimens including 46 subjected to cyclic increasing loads. The data cover 105 to 405 kg/cm<sup>2</sup> of concrete strength, 0 to 1.49 % of web reinforcement ratio, 1.0 to 7.5 of ratio of unsupported length

to depth of column and 0 to 233 kg/cm<sup>2</sup> of average axial stress.

3. Shear strength equation for reinforced concrete columns

It has been known that the shear strength of columns has a tendency to increase as the magnitude of the introduced axial force increases. The ratios of the test data available for strength to the calculated results from Eq.(1) and Eq.(2) are plotted in Fig.4, where unsupported length of column, h<sub>0</sub>, is substituted for 'a' in the equations. In Fig.4, the differences between the monotonic increase and the repeated reversal of loading, and between the simple beam type and the other type of loading are not obviously observed.

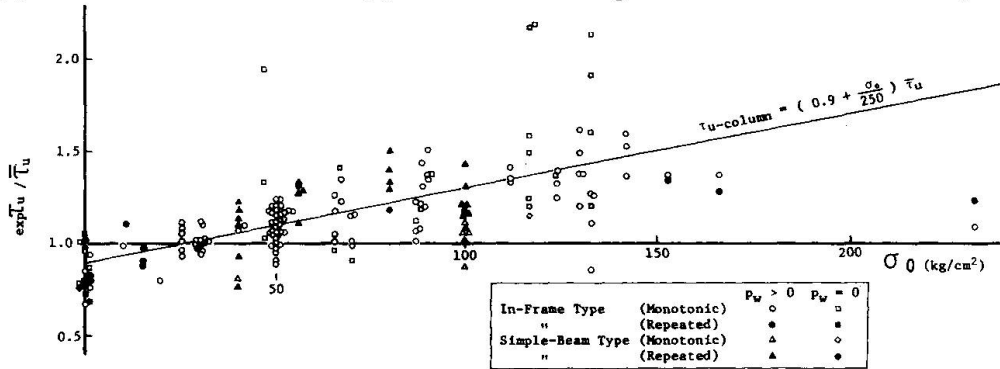


Fig. 4

The following equation is derived from the average line of the plots as an empirical equation for the ultimate shear strength of columns:

$$\tau_{u-column} = (0.9 + \frac{\sigma_0}{250}) \bar{\tau}_u, \quad \text{in kg/cm}^2 \quad (3)$$

where

$\sigma_0 = P/bD =$  average compressive stress of column.

$\bar{\tau}_u =$  calculated value from Eq.(1) or Eq.(2) by substituting unsupported length of column, h<sub>0</sub>, for 'a' in the equation.

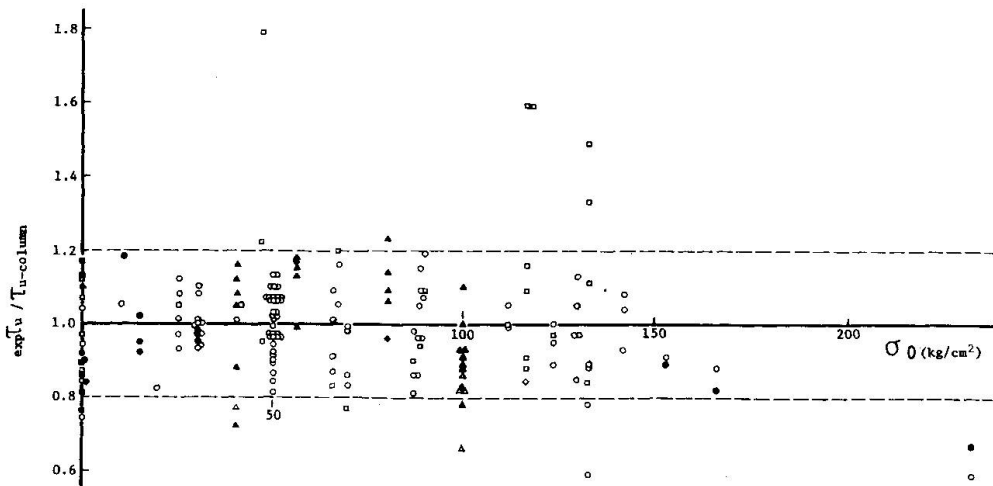


Fig. 5

The comparison of the test data with the calculated results from the proposed equation is shown in Fig.5, where 89.7 % of all the plots falls within the range of  $\pm 20\%$  of the calculated values. The mean value of the ratio  $\tau_{exp} / \tau_{u-column}$  and the standard deviation in each category of loading is presented in Table 3. Far deviated plots in Fig.5 are mostly of specimens without web reinforce-

ment. In practice, columns are usually provided with some amount of web reinforcement and subjected to axial stresses less than about 100 kg/cm<sup>2</sup>. Under the limitation of  $p_w > 0$  and  $\sigma_o \leq 100$  kg/cm<sup>2</sup>, the mean of the ratios of the test data to Eq.(3) and the standard deviation are shown in Table 4. The data within the range of  $\pm 20\%$  from Eq.(3) are 96 % of the total. Considering the variety of the test programs, it may be said that Eq.(3) is satisfactory in accuracy and for the practical evaluation of the ultimate shear strength of columns.

Table 3

Category (whole data)	Number of data	Mean of the ratios	Standard deviation
Total	175	0.991	0.158
Monotonic	130	0.995	0.164
Repeated	45	0.980	0.139
Simple-beam type	33	0.972	0.151
In-frame type	142	0.996	0.159

Table 4

Category ( $p_w > 0$ $\sigma_o \leq 100$ )	Number of data	Mean of the ratios	Standard deviation
Total	119	0.988	0.111
Monotonic	84	0.982	0.105
Repeated	35	1.003	0.124

#### 4. Lateral deformability of columns at shear failure

The observed deformation consists of two components, flexural and shear, in the test data. As the details of the specimens, the properties of materials and the levels of the acted bending moment at the shear failure are considerably different among the investigators, it is desirable to separate the shear deformation from the flexural deformation, if possible. The flexural deformation cannot, however, be evaluated on the flexural theory of continuum after various patterns of shear cracks have distinctly occurred, or after the bond between axial reinforcement and concrete has been released. For the above reason, it seems rather irrational to distinguish their shares in the observed deformation. The deformability cannot but be treated here as the ability of the whole lateral deformation of columns. The data are widely scattered under any limited condition, so that we proceed with the discussion on the lowest values of the scatters. The effects of four influencing factors, i.e. concrete strength, web reinforcement ratio, ratio of unsupported length to depth of column and average axial stress, are examined respectively, and the following tendencies of the lowest values of the scatters are observed. The lateral deformability of columns will be the smaller, (1) the higher the strength of concrete is, (2) the lower the web reinforcement ratio is, (3) the smaller the ratio of unsupported length to depth of column is, (4) the larger the average axial stress is. The data of 185 specimens are divided into three groups according to the levels of axial stresses, and the equations are obtained as the expressions of the lowest-limit-lines, respectively.

$$\left. \begin{aligned} 0 \leq \sigma_o < 40 \text{ kg/cm}^2 & \quad \min R_{u1} = 2p_w (h_o/D) \left( 1 + \frac{300}{f'_c} \right) \\ 40 \leq \sigma_o < 100 & \quad \min R_{u2} = 1.5p_w (h_o/D) \left( 1 + \frac{300}{f'_c} \right) \end{aligned} \right\} (4)$$



$$100 \leq \sigma_o \leq 233 \quad \min R_{u3} = p_w (h_o/D) \left( 1 + \frac{300}{f_c} \right)$$

where  $R_u = \delta_u / h_o =$  ultimate deflection angle of column.  
 $\delta_u =$  ultimate lateral deflection of column.

On the assumption that these equations correspond to the middle values of the respective ranges of axial stresses, the relation between the minimum deformation and the regarding factors are consolidated into an equation.

$$R_{u-\min} = p_w (h_o/D) \left( 1 + \frac{300}{f_c} \right) \left( \frac{500}{\sigma_o + 180} - 0.5 \right), \text{ in } 10^{-3} \text{ rad.} \quad (5)$$

The comparison of the test data with Eq.(5) is plotted in Fig.6. Only five plots fall below Eq.(5). The difference between two types of loading, monotonic and repeated, is not obviously observed in Fig.6. In spite of the indistinctness of its physical meaning, Eq.(5) would be useful for assessment of the minimum of the lateral deformability of columns at shear failure for the present until a more rational method is established.

In the design of structural members, it should be intended that the brittle failure such as shear failure might not occur in the ultimate state, so as to insure the ductility of structures. This ought to be brought about by making the flexural strength of members less than the shear strength. The shear strength of columns would be assessed from Eq.(3).

In the case where the shear strength is inevitably less than the flexural strength, the column should be endowed with the sufficient deformability to follow the response lateral deformation of the whole structure. The Eq.(5) would be utilized as a measure for evaluation of the deformability.

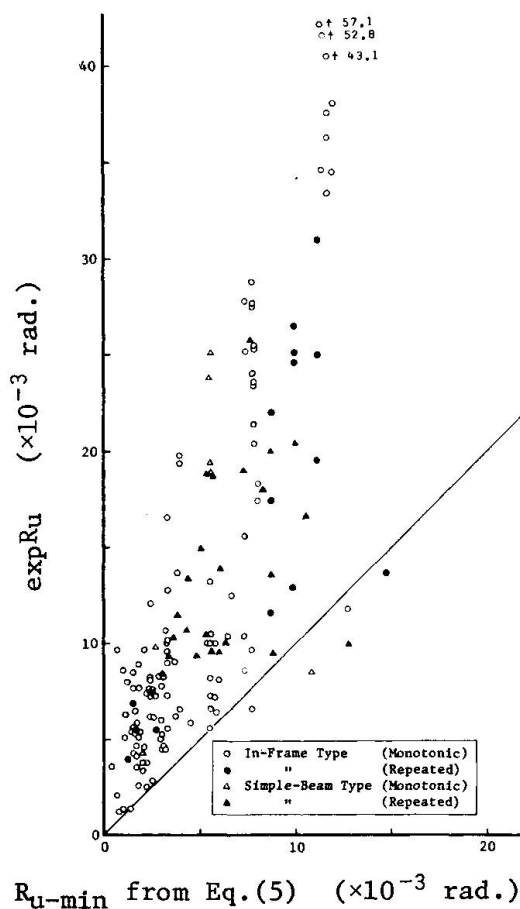


Fig. 6

## SUMMARY

The equations to assess the shear strength and the ultimate lateral deformability at shear failure of reinforced concrete columns are proposed. These equations are derived from the investigation of the test data which have been presented in Japan since 1961. The differences between two types of loading, monotonic increase and repeated reversal, are obscure in the shear strength or the ultimate lateral deformability.

## RESUME

On propose dans ce travail les équations pour évaluer la résistance au cisaillement et la déformabilité latérale ultime au moment de la rupture par cisaillement de colonnes en béton armé. Ces équations sont dérivées de l'étude des résultats d'essais présentés au Japon depuis 1961. Les différences entre deux types de charge, charge monotone et charge répétée alternée, sont dévoilées par la résistance aux efforts de cisaillement et par la déformabilité latérale ultime.

## ZUSAMMENFASSUNG

Es werden die Gleichungen zum Abschätzen des Schubwiderstandes und der horizontalen Auslenkung beim Schubbruch von Stahlbetonstützen vorgeschlagen. Diese Gleichungen werden aus der Untersuchung von Testdaten abgeleitet, die in Japan seit 1961 veröffentlicht werden. Die Unterschiede zwischen zwei Belastungsarten, stetig zunehmend und wiederholt wechselnd, sind hinsichtlich des Schubwiderstandes und horizontaler Bruchverformbarkeit unklar.



Leere Seite  
Blank page  
Page vide

## IV

### Local Bond Stress-Slip Relationship under Repeated Loading

Relation tension/glissement dans les attaches locales soumises à des charges répétées

Lokale Haftspannung/Gleitung-Beziehung unter wiederholter Belastung

**Shiro MORITA**

Associate Professor

Dept. of Architectural Engrg.

Kyoto University, Japan

**Tetsuzo KAKU**

Research Associate

Dept. of Architectural Engrg.

#### 1. Introduction

It is well known that the bond deterioration between steel and concrete is a significant factor influencing the behavior of reinforced concrete structures under actions of repeated working loads, and also reversed cyclic overloads expected from strong motion earthquakes [1]. Though many studies have shown the stiffness deterioration characteristics of reinforced concrete members under cyclic loading, in most cases the influences of the bond deterioration on the behavior have not been studied extensively.

The ultimate objective of this investigation is to determine the analytical method for predicting the role of bond in the behavior of reinforced concrete structures under load reversals, on the basis of the experimentally determined basic law of bond deterioration. In this investigation reported herein the effect of the load history on the local bond-slip relation was studied from the pull- and push-out tests of the specimens having reinforcing steel bonded to concrete in a short length. Using the derived law of bond-slip, bond stress distribution along reinforcement in axially reinforced concrete prisms subjected to cyclic loads was calculated to explain the mechanism of hysteretic load-deformation curves of reinforced concrete members.

#### 2. Experimental Study on the Local Bond-Slip Relationship

The hypothesis that the steel stress or strain distribution along reinforcement embedded in concrete can be determined from the basic law of local bond stress-slip relationship, has been confirmed by many researchers. Though it is difficult to measure not only local bond stress but also local slip, several test methods have been successfully developed [2,3]. In this study, the method introduced by Rehm [2] was used to various loadings including load reversals.

Test Specimen As shown in Fig. 1, five reinforcing bars for bond tests were embedded in a short reinforced concrete beam at right angles to its axis and were held in a vertical position at concrete casting. Each bar was contacted effectively with concrete in the

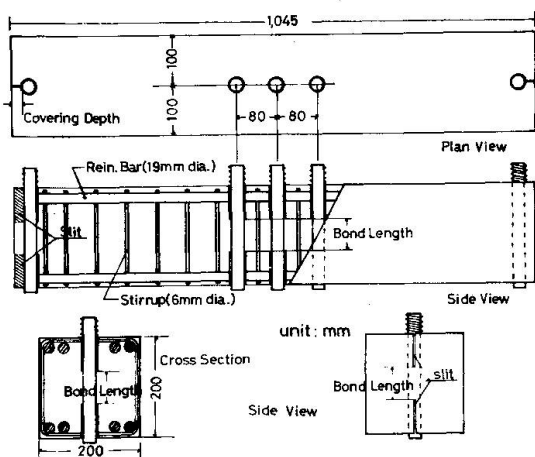


Fig. 1. TEST SPECIMEN

levels. Slits were provided for concrete cover at the outside of the bond zone of these two bars; otherwise concrete cover at these parts might resist together to the wedging action of the bar within the bond zone. Test series of these bars embedded at the beam ends was referred to as "Series B". The nominal dimensions of the test specimen are indicated in Fig. 1. Deformed bars of 19 and of 25mm diameter were used in the tests and the bond length of 48mm for 19mm diameter bars, and of 66mm for 25mm diameter bars was provided. The depth of concrete cover for bars in Series B was held constant at 20mm. The concrete was a blend of Portland cement (1 part), river sand (2 parts) and river gravel (3 parts) with a maximum size of 20 mm. Water-cement ratio was 53% and the concrete strength  $f_c'$  at the time of loading tests (at 41 to 76 days after casting) varied from 305 to 347 kg/cm<sup>2</sup>. Loading tests were performed on 18 bars of 25mm diam. and 12 bars of 19mm dia. in Series A, and on 8 bars of 25mm diam. in Series B.

**Test Setup** Loads were applied by Instron type testing machine of  $\pm 50$  ton maximum capacity to the threaded end of the bar. Fig. 2 shows the loading arrangement for both series; the reinforced concrete beam acted as a simply supported beam in Series A and as a cantilever beam in Series B.

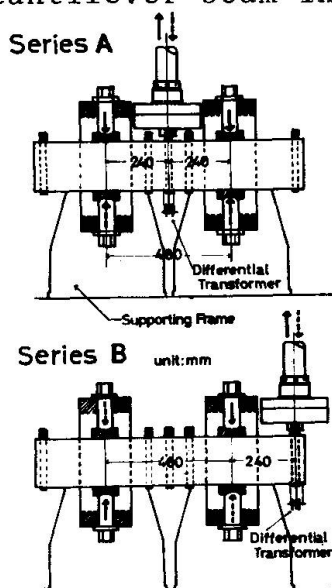


Fig. 2. LOADING ARRANGEMENT

bond length of two times the pitch of transverse ribs. The bond zone was located at midheight of the beam to avoid the influence of the flexural stress of the beam. Since the bond zone for three bars at the central part of the beam was located deeply inside the concrete block, high bond stress was expected with the increase of the local slip. Test series of these bars was referred to as "Series A". On the other hand, two bars at the beam ends were located near the concrete surface, and serious damage of bond due to the formation of a longitudinal crack along the bar was expected at large slip

measured by a differential transformer and cross-head speed of testing machine was controlled mostly at 1.0 mm/min. The out-put of the load cell and the output of end slip were fed into the X-Y recorder of the testing machine.

**Load Histories** The influence of various load histories on the bond-slip behavior was examined. In every loading histories the direction of loading was also a significant factor. Therefore, the upward direction (bar in tension) was defined as positive and downward (bar in compression) as negative. Selected loading histories were assorted as follows;

- MN... Monotonic loading to failure.
- RP... Repeated loading in one direction with an additional slip in each cycle.
- RV... Reversed (bi-directional) loading with an additional slip in each cycle.
- RL... Cyclic reversed loading between constant load limits.

RS... Cyclic reversed loading between constant slip limits. In these tests the slip limits were increased mostly after 10 cycles of the previous slip range.

RR... Repeated or reversed loading in a random manner in order to confirm the derived basic bond-slip law.

Designation of Test Specimen For example, the notation A 25-6-RS indicates the following characteristics.

- A: Test Series A
- 25: Bar diameter of 25mm
- 6: Number of the bar
- RS: Load history RS

Test Results Under the assumption that bond stress distributes uniformly along the bar axis within the bond zone, the local average unit bond stress and the local average slip could be obtained from the test data. Because the differences between the free end slip and the average slip were negligibly small even at a high stress level, the experimentally obtained end slip was assumed to be equal to the local slip without modification. From the above mentioned approximation, each experimental curve was transformed to the local bond-slip curve.

In Fig. 3, the bond-slip curves under monotonic loading in either direction are shown. Each one represents the average curve of the results obtained on the specimens having the same characteristics. Fig. 3 shows that the loading direction gave a significant influence on the slope of the bond-slip curve at a relatively low bond stress level, and that a marked reduction in the maximum bond stress and a gradual decrease of bond stress with the further increase of slip were produced in Series B as expected.

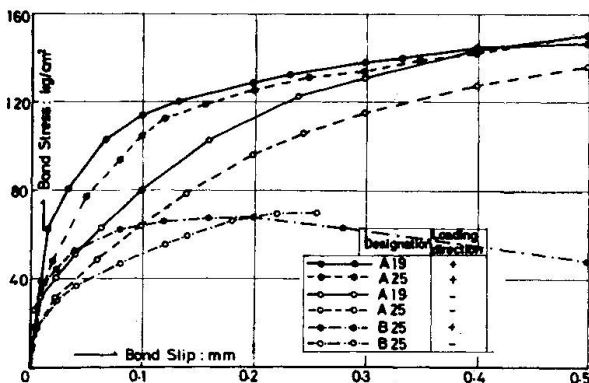


Fig. 3. BOND-SLIP CURVES UNDER MONO. LOADING

Typical test results of the bond stress-slip relationship under load repetitions or reversals are shown by solid lines in Fig. 4 (a)-(g). It could be pointed out as the general characteristics throughout the test results that a small number of repetition within a limited slip range did not give a significant effect on the bond-slip behavior at a larger slip than the peak slip in the previous cycles and, on the other hand, once the peak slip was increased, a considerable reduction in bond was produced at a lower slip in the subsequent load history. These behaviors were also indicated in the previous studies [4.5]. Fig. 5 shows the bond deterioration due to cyclic loading between limit slips. In this figure the ratio of the peak bond stress at each of successive cycles to that at the first cycle ("bond deterioration ratio") was plotted against number of cycles. Fig. 5 indicates that parameters, such as bar diameter, the loading direction, the previous loading history within a lower

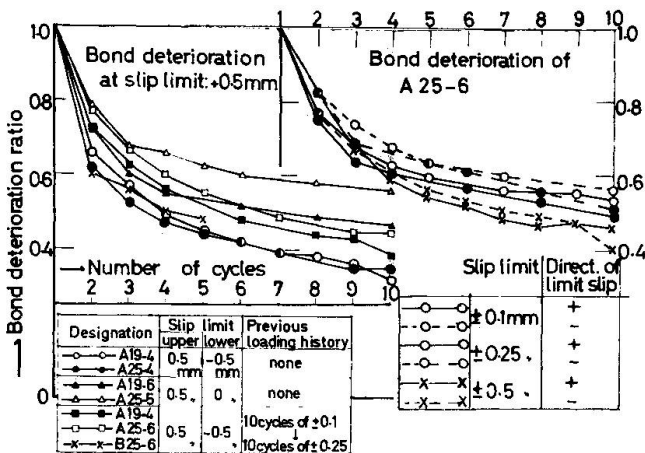


Fig. 5. THE BOND DETERIORATION RATIO (RS Tests)

Slip limit and the magnitude of slip limit, did not give any sensitive influences upon the bond deterioration ratio.

3. The Bond-Slip Law under Repeated Loading

From the experimental results of the bond-slip behavior under various load histories, it was attempted to derive the basic law of local bond-slip relationship. As a first approximation at this phase of the study, a highly simplified law was presented.

**Envelope Curve** The envelope curve was defined as the bond-slip curve obtained under monotonic loading to failure and approximated by the bi-linear relationship as shown in Fig. 6 within the slip range of  $\pm 0.5$ mm.

**Unloading and Reversed Loading Curves** The assumed law for these curves is schematically explained in Fig. 7. The stiffness  $K_3$  of linear unloading and the coefficients  $\alpha$  and  $\beta_x$ , which define the magnitude of bond deterioration, were determined on the basis of the test results. The values of  $K_3$ ,  $\alpha$  and  $\beta_x$  were the following;

$$\begin{aligned}
 K_3 &= 4 \cdot 10^4 \text{ kg/cm}^3 & (1) \\
 \alpha &= 0.18 & (2) \\
 \beta_x &= 0.9 \quad \text{for } S_x < 5 \cdot 10^{-3} \text{ cm} \\
 &= 0.9 - 4.44 (S_x - 5 \cdot 10^{-3}) \\
 &\quad \text{for } 5 \cdot 10^{-3} \text{ cm} < S_x < 5 \cdot 10^{-2} \text{ cm} & (3)
 \end{aligned}$$

where  $S_x$  in Eq.(3) indicates the slip value of the point x from which unloading is started.

Applying the law shown in Fig. 7 repeatedly, the bond-slip response

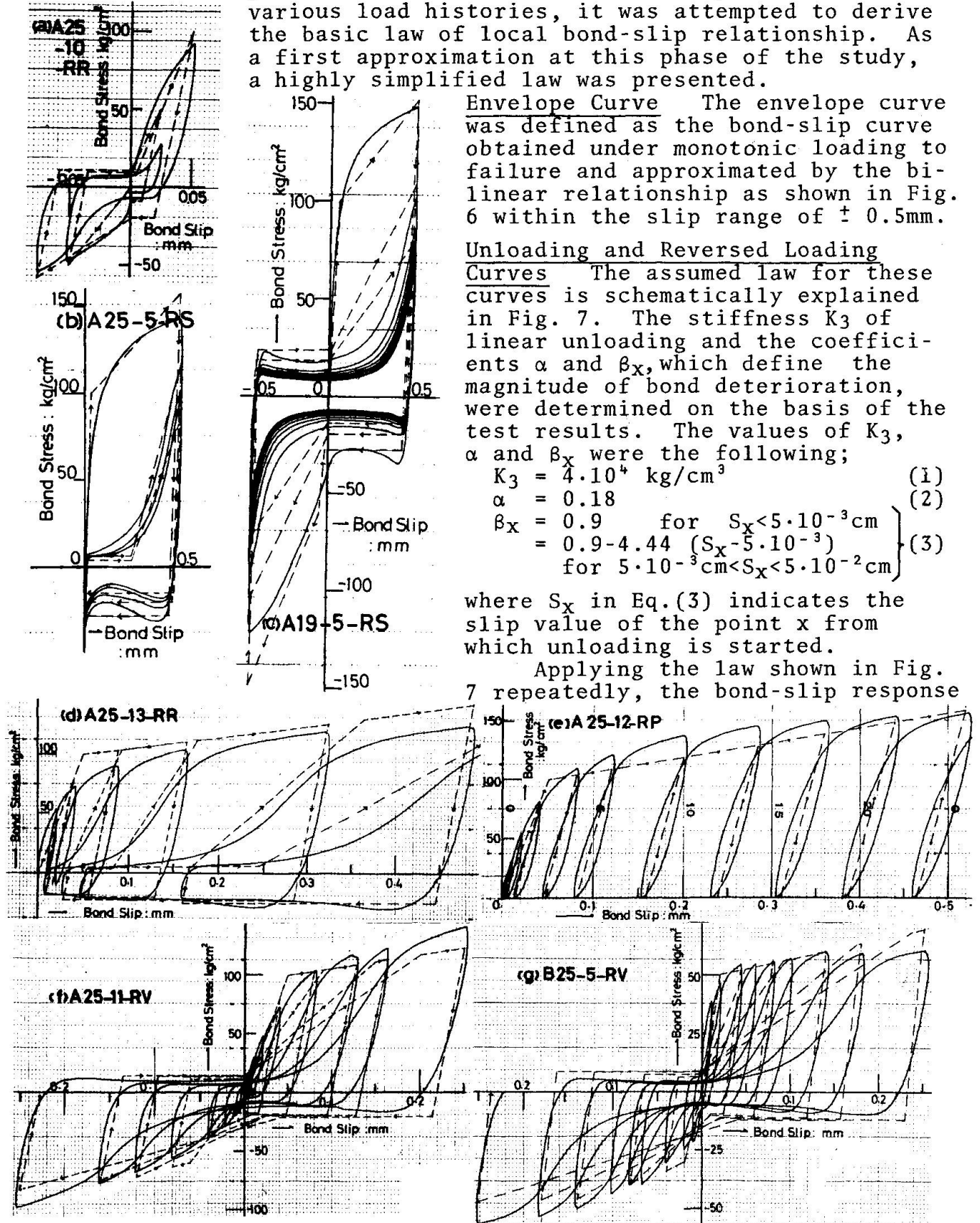
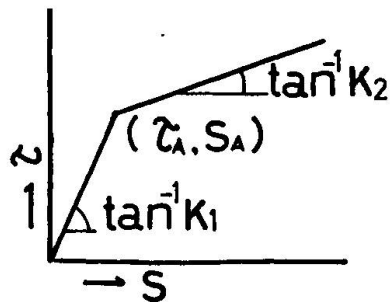


Fig. 4. BOND-SLIP CURVES UNDER VARIOUS LOAD HISTORIES



could be computed for the slip histories imposed to each specimen. These curves are shown in Fig. 4 by broken lines along with the experimental curves. The agreement of both curves seems to be fairly well. However, in the case of the cyclic loading tests between constant slip limits (Fig. 4(b),(c)), the bond deterioration at the peak slip is overestimated with the increase of the number of cycles. The main reason of this is that the coefficient  $\beta_x$  given by Eq.(3) varies not only with the slip  $S_x$  at the start of unloading, but also with the number of cycles. The law of bond-slip behavior assumed in this study must be improved in the advanced phase of the study.

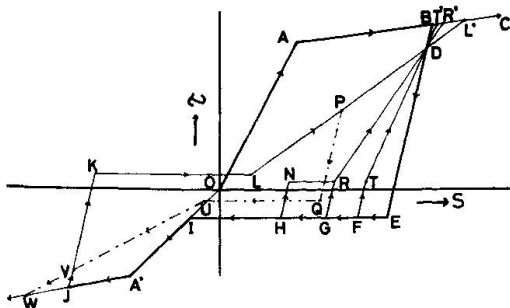
4. Application of the Basic Law of Bond-Slip



Test series	Loading direction	$z_a$ (mm)	$S_a$ (mm)	$K_1$ ( $\times 10^4 \text{ kg/cm}^2$ )	$K_2$ ( $\times 10^4 \text{ kg/cm}^2$ )
A	+	100	0.05	2.0	1.10
	-	60	0.06	1.0	2.05
B	+	50	0.02	2.5	0.83
	-	30	0.02	1.5	1.94

Fig. 6. APPROXIMATION OF ENVELOPE CURVES

As the typical examples, the behaviors of the ordinary pull-out specimen and the tension specimen under repeated loading were calculated. Assuming that the axial stress in concrete distributes uniformly in a cross section and the shear deformation can be neglected, the distributions of local slip, bond stress and steel stress were calculated as a one-dimensional problem. An iterative method was used by dividing the embedded length of the bar into short elements (15 elements of equal length for the pull-out specimen and 20 for the tension specimen). Fig. 8 shows the applied load versus end slip curve of the pull-out specimen of which the dimension also shown in the figure. In this example, the envelope curve in the positive direction of Series A was used in both directions. It is noteworthy that the response of the typical hardening type can be seen under the action of load reversals between excessive slip limits. Fig. 9 shows that the hysteretic behavior of the tension specimen, similar to the results of previous studies [3,4], can be predicted on the basis of the local bond-slip law. It should be noted in this example that tensile stress transferred to concrete is enough to form a crack at the mid-span at 5 ton or the less, but the formation of crack is not considered throughout the opposed history.



$$\begin{aligned}
 z_D &= A_0 z_B & S_D &= S_B - (1 - A_1) z_B / K_1 & z_E &= z_F = z_G = z_H = z_I = -\alpha z_B \\
 S_E &= S_B - (1 + \alpha) z_B / K_1 & S_O &= S_B / 2 & z_T &= z_R = z_N = -\alpha z_E \\
 S_R &= S_B / 2 - (1 + \alpha) z_B / K_1 & S_T &= S_F - (1 + \alpha) z_F / K_1 & z_K &= -\alpha z_I \\
 S_N &= S_H - (1 + \alpha) z_H / K_1 & S_K &= S_U - (1 + \alpha) z_U / K_1 & S_L &= (S_B + S_U) / 2 \\
 S_O &= S_P - (1 + \alpha) z_P / K_1 & S_V &= S_U - (1 - A_2) z_U / K_1 & S_U &= (S_U + S_P) / 2 \\
 z_Q &= -\alpha z_P & z_V &= A_2 z_U & & & A_1 \text{ and } A_2 \text{ are given from Eq.(3)}
 \end{aligned}$$

Example to follow the law of loops.

Consider that unloading is started at an arbitrary point ( $z, S$ ) lying on the curve (EIA'W).

- Range of S at unloading point Example of subsequent route
- $S > S_C$  - - - - - F-T-D-T'-C
- $S < S_C$  and  $S_R < (S + S_B) / 2$  - - - H-N-R-D-R'-C
- $S < S_C$  and  $S_R > (S + S_B) / 2$  - - - J-K-L-D-L'-C

Fig. 7. BASIC BOND-SLIP LAW

5. Conclusions

The following conclusions were obtained; (1) The deterioration of local bond depends on the magnitude of the previous maximum local slip, and the larger the previous slip the greater is the reduction in bond stress at lower slip levels. (2) The deterioration of peak bond stress under cyclic loading between constant slip limits is rather moderate as shown in Fig. 5.

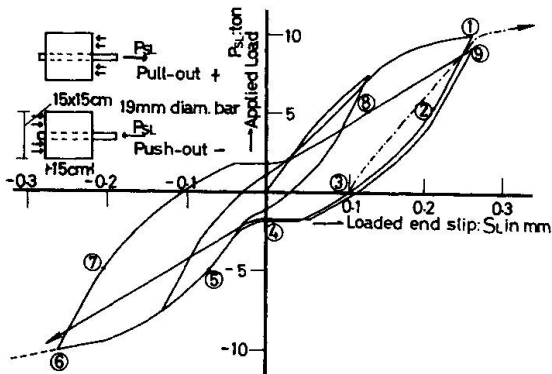


Fig. 8. COMPUTED BEHAVIOR OF THE PULL-OUT SPECIMEN

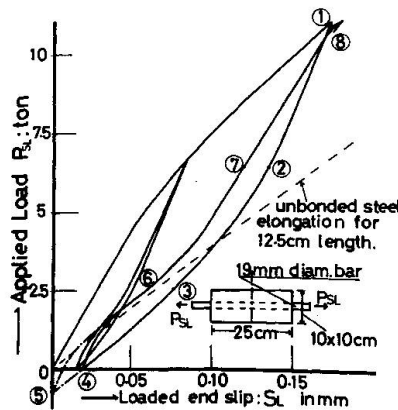


Fig. 9. COMPUTED BEHAVIOR OF THE TENS. SPECIMEN

(3) The proposed model of the local bond-slip law provides a satisfactory agreement with the test results under various load histories. (4) The load-deformation characteristics of reinforced concrete members can be predicted by use of the basic law.

#### [References]

- [1] Bertero, V., and Bresler, B., "Seismic Behavior of Reinforced Concrete Framed Structures", Proceedings of 4th WCEE, Chile, 1969, Vol.1.
- [2] Rehm, G., "Über die Grundlagen des Verbundes zwischen Stahl und Beton", Deutscher Ausschuss für Stahlbeton, H.138, 1961
- [3] Morita, S., et al, "Fundamental Study on Bond between Steel and Concrete", Trans. of the A.I.J. No.131, 132, 134 & 139, 1967.
- [4] Bresler, B., and Bertero, V., "Behavior of Reinforced Concrete under Repeated Load" Proc. of the ASCE, ST 6, June, 1968.
- [5] Ismail, M., and Jirsa, J., "Bond Deterioration in Reinforced Concrete Subjected to Low Cycle Loads", ACI Journal, Proc. Vol.69, No.6, June, 1972.

#### SUMMARY

The effect of the load histories on the local bond-slip relationship was studied from the pull- and push-out tests of reinforcing bars effectively contacted with concrete in a short length. From the test results the basic bond-slip law was derived and applied successfully to the prediction of the behavior of reinforced concrete members under load reversals.

#### RESUME

On a étudié l'influence du processus de charge sur la relation entre la liaison locale et le glissement de fers d'armature en contact avec le béton sur une petite longueur au moyen d'essais d'extraction et d'essais d'enfoncement.

De ces essais on a dérivé la loi de base liaison-glissement et elle a été appliquée avec succès pour l'étude du comportement d'éléments en béton armé soumis à des inversions de charges.

## ZUSAMMENFASSUNG

Der Einfluss der Belastungsarten auf das lokale Haft-Schlupf-Verhalten wurde anhand von Zug- und Hinausdrück-Versuchen an Armierungsstäben untersucht, deren Verbund mit dem Beton nur auf eine kurze Strecke gewährleistet war. Von den Versuchsergebnissen wurde das grundlegende Haft-Schlupf Gesetz abgeleitet und erfolgreich zur Voraussage des Verhaltens von Stahlbetonteilen unter Lastumkehr angewendet.



Leere Seite  
Blank page  
Page vide

## IV

### Strength Increase under Repeated Loading

Augmentation de résistance sous charges répétées

Festigkeitszunahme unter wiederholter Belastung

Milík TICHÝ      Vladimír URBAN  
Building Research Institute  
Technical University in Prague  
CSSR

As a part of a research of the low-cyclic loading effects in concrete structures, tests of 4 sets of prestressed pretensioned beams have been performed with the aim to establish the effect of very high overload on the ultimate strength, deformation, crack initiation, propagation and possibly also other parameters.

Each set consisted of 30 nominally identical beams pretensioned by strands  $3 \times \emptyset 3$  mm (steel 140/170 kp/mm<sup>2</sup>), the mean strength of concrete was 400 kp/cm<sup>2</sup> (cubes 20x20x20 cm). The sets differed by the amount of reinforcement and by presence or absence of prestressing strands in the compression zone (Fig.1a). The total depth of cross section was varied in each set to ensure zero stresses in extreme fibres of concrete in the unloaded state. The test scheme is shown in Fig.1b.

Ten beams (group I) of each set were subjected to monotonously increasing load up to the failure and the mean strength  $\bar{F}_{u1}$  was calculated. The remaining beams were tested in two equal groups II and III. These beams were subjected primarily to the load  $F_0 = \alpha \cdot \bar{F}_{u1}$  (with  $\alpha_{II} = 0,86$  and  $\alpha_{III} = 0,92$  for group II and III, respectively), then they were unloaded and again reloaded up to the failure load  $\bar{F}_{u2}$ . The loading was controlled by constant deflection increment at the midspan. The loading history is illustrated in Fig.2. A complete record of measured values was obtained during experiment. Following quantities were

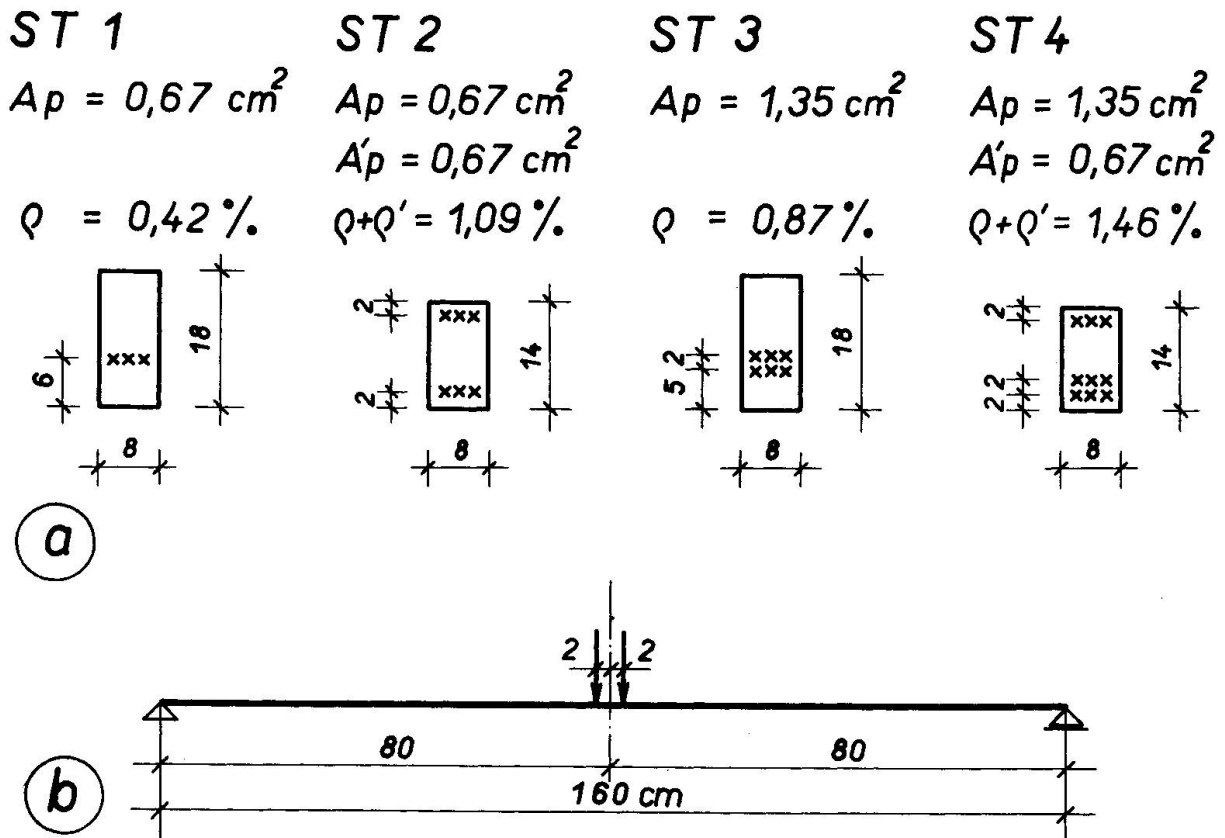


Fig.1. (a) Cross-section of specimens  
(b) Test scheme

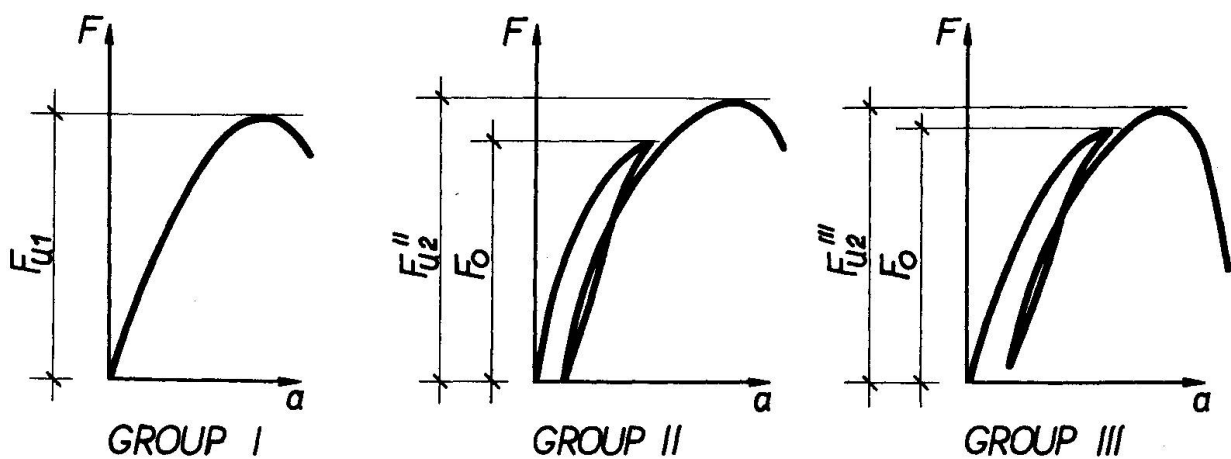


Fig.2. Loading history

measured: load, deflection at midspan, slopes at support sections, bottom fibre strain and compressive and transverse strain of upper fibres. The initiation, propagation and width of cracks were also recorded. Material properties of beams were evaluated before test and also on specimens cut out of beams after failure.

The results show that the load carrying capacity  $\bar{F}_{u2}$  of beams is affected by the initial loading to the value  $F_0$  as can be seen from Fig.3. It has been observed in sets ST1, ST3, ST4 (see Fig.3a,c,d) that the initial loading increased the load carrying capacity. Only the ST2 set indicates load carrying capacity decrease (Fig.3b).

The experimental data were statistically processed. The values of statistical parameters of strength for all groups of beams are shown in Tab.1.

SET	ST 1			ST 2			ST 3			ST 4		
GROUP	I	II	III	I	II	III	I	II	III	I	II	III
$\bar{F}_{u1}$ (kp)	2532	-	-	2465	-	-	4303	-	-	3547	-	-
$\alpha$	0,0	0,86	0,92	0,0	0,86	0,92	0,0	0,86	0,92	0,0	0,86	0,92
$\bar{F}_{u2}$ (kp)	-	2539	2824	-	2319	2431	-	4500	4414	-	3702	3740
$\bar{F}_{u2}/\bar{F}_{u1}$ %	100,0	100,3	111,6	100,0	94,1	98,6	100,0	104,6	102,6	100,0	104,4	105,4
$\sigma$	149,8	174,8	142,1	195,7	152,9	194,0	230,2	259,9	199,5	320,9	259,9	202,5
$\nu$	0,059	0,069	0,050	0,079	0,066	0,081	0,054	0,058	0,045	0,090	0,070	0,054

Tab.1. Statistical parameters:

$\bar{F}_{u1}$  - mean strength of group I,  $\bar{F}_{u2}$  - mean strength of group II and III respectively,  $\alpha = F_0/\bar{F}_{u1}$  ( $F_0$  - initial load),  $\sigma$  - standard deviation,  $\nu$  - coefficient of variation

The increase of strength due to the first loading can be clarified by the hypothesis of cyclic strengthening as follows:

Let us consider an element of rectangular cross-section and subjected to bending. Let it be reinforced or prestressed in such a way that under single application of load it would fail by crushing of concrete as soon as the ultimate moment in the cross-section under the load has been attained. Hence, the stress at

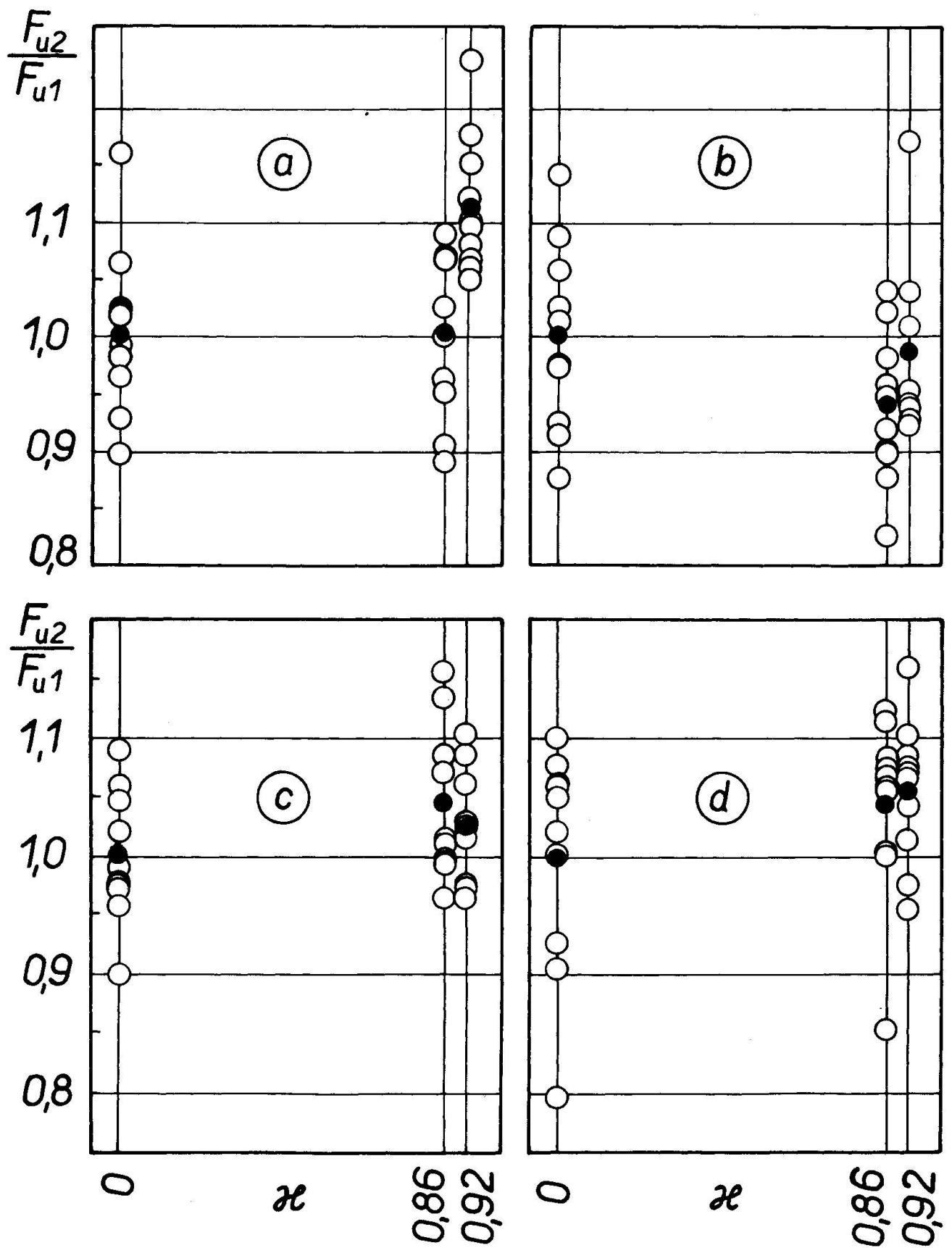


Fig.3. Ultimate strength of specimens  
 (a) - ST1, (b) - ST2, (c) - ST3, (d) - ST4

failure in the reinforcement is lower than the yield stress or the strength of the reinforcement.

Let this element be loaded by a load  $F_0 < F_u$  (where  $F_u$  is the ultimate strength of the element) in such a way as to produce at least a partial plastic deformation in concrete. Under the load the depth of the compression zone is  $x_0 > x_u$  (where  $x_u$  is the depth due to  $F_u$  - see Fig.4). Now, if the element is unloaded, structural changes due to plastic deformation of concrete take place, which may after several repetitions of the load produce partial or total separation of the tension and of the compression zone. Due to this the deformation compatibility of the cross-section will have been substantially reduced and the deformation of the compression concrete is no more geometrically dependent on the deformation of the reinforcement. The element behaves now like a tied arch. The thickness of the concrete part of the arch is  $x_0$ .

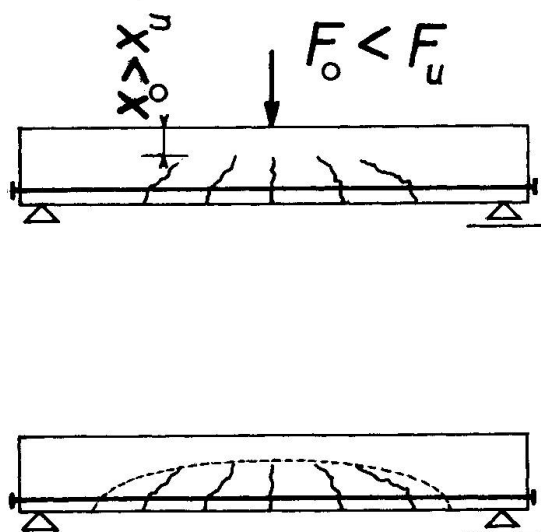


Fig.4. Pattern of failure

The arch behaviour does not change even when the load increases to  $F > F_0$ , the concrete part of the girder being subjected only to compressive stresses. When the ultimate strength of the element is attained, the force acting in the concrete is

$$C = f_c b x_0$$

where  $f_c$  is the compressive strength of concrete and  $b$  the breadth of the cross-section. Owing to the fact that

$x_0 > x_u$  the force  $C$  and consequently also the force  $T$  acting in the reinforcement must be higher than at the ultimate strength

under single application of load. Hence, after preceding repeated loading the ultimate moment  $M_{un}$  is higher than the ultimate moment under a single load application. Assuming the stress in the compression zone as constant, it follows that

$$\frac{M_{un}}{M_u} = \frac{x_o}{x_u}$$

The increase of the ultimate strength of the element has been produced by the change of its structural response.

Obviously, the strength increase can be produced only in elements with compression failure where an increase of the stress in the reinforcement is possible. In elements with tension failure (failing by excessive elongation or by rupture of the reinforcement) the implication of the presented hypothesis would be the reductiva of ultimate strength.

#### SUMMARY

The effect of overloading on the subsequent load carrying capacity of prestressed concrete beams was experimentally investigated on 120 specimens of four types of cross-section and reinforcement. Statistically processed data indicate that initial load near to the ultimate load increases the subsequent bending strength. A hypothesis of cyclic strengthening is submitted.

#### RESUME

L'influence de surchargement sur la résistance postérieure de poutres en béton armé a été étudié expérimentalement sur 120 spécimens de 4 types d'armature et de sections différentes. Les résultats traités statistiquement montrent qu'une charge initiale proche de la charge ultime augmente la résistance à la flexion. On propose une hypothèse d'augmentation de résistance cyclique.

#### ZUSAMMENFASSUNG

Der Einfluss von Ueberbelastung auf die spätere Tragkapazität vorgespannter Betonbalken wurde anhand von 120 Beispielen von vier Querschnittstypen und Bewehrungsarten untersucht. Statistisches Vorgehen bei der Auswertung der Versuchswerte zeigt, dass die anfängliche Last nahe der Traglast den späteren Biegewiderstand erhöht. Eine Hypothese über zyklische Verstärkung wird angegeben.



## IV

### **Transient Deformation Behaviours of Prestressed Concrete Beams under Repeated Over-load**

Comportement de déformation momentanée des poutres en béton précontraint soumises à des surcharges répétées

Vorübergehendes Deformationsverhalten vorgespannter Betonbalken unter Schwellbelastung

**Hiroshi MUGURUMA**      **Megumi TOMINAGA**  
Professor                      Associate Professor  
of Architectural Engineering  
Kyoto University, Japan

**Yoshitada TAKAYA**      **Toshimasa TADA**  
Graduate student              Graduate student  
Kyoto University, Japan

### Introduction

The prestressed concrete members or frames must have the stabilized properties under the repeated over-loads developed during heavy earthquakes. That is, their deterioration mechanisms under the repeated over-load should be clarified. It may be considered that the transient deteriorations of prestressed concrete members under the repeated over-load are mainly caused from both the deterioration of concrete in compression side and bonding ability of grout and the permanent strain set of prestressing steel. The basic properties of these factors under repeated over-load are not sufficiently clarified to predict the transient behaviors of the prestressed concrete members. Therefore, this study aims to obtain the knowledges of overall trends by an experimental approach.

### TEST RESULTS UNDER THE NON-REVERSED REPEATED LOADS

Firstly, the transient flexural behaviors under the non-reversed repeated over-load were investigated. Main interest was focussed in the change of moment-curvature relationship during cyclic load.

#### Test beams

Test beams were cast with the synthetic lightweight aggregate concrete and grouted with cement paste after prestress transferring. The dimensions and details of test beams are shown in Fig. 1 (a). The prestressing tendon was of 16mm dia. and located at the distance of one-sixth the total depth of beam from the centroid and tensioned to the allowable stress which produced stress of one-third the compressive strength of concrete in the compression side and almost zero in the opposite side. Unless specified, the specimens had stirrups of 6mm dia. at the intervals of 150mm and two erection bars of 6mm dia. in each of compression and tension side of the section. Employed prestressing tendons were smooth round bars treated by high frequency induced heat.

### Effect of load intensity

The first factor considered was the load intensity at the instant of reloading, which was eventually expressed by the compressive extreme fiber strain  $\epsilon_{c.ul}$  of concrete, such as 1.8, 2.0, 2.2, 2.4, 2.6 or 2.8%. The moment  $M$ -curvature  $\phi$  relations under the loading history, including one cycle of complete loading and unloading between zero to the specified load level and again reloading until failure, were compared with those under the simple loading. Fig. 1 (a) to (c) show the changes of the moment-curvature relations during the loading, unloading and reloading stages respectively, which are given in non-dimensional expression by dividing with the theoretical values of  $M$  and  $\phi$  for the monotonous loading. Likewise, the non-dimensional flexural stiffness-moment relations are briefly represented in Fig. 2 in which the solid line is for simple loading. Since the breaking points showing the degradation of stiffness seem to lie at almost the same moment, these degraded stiffnesses were plotted against the strain  $\epsilon_{c.ul}$  as shown in Fig. 3. This figure shows that the compressive extreme fiber strain  $\epsilon_{c.ul}$  of concrete at the beginning of reloading is useful as the factor governing the stiffness degrading of prestressed concrete beams. To residual curvature and decompression moment similar principle was applied, thus the calculated moment-curvature curve showed the considerably good agreement with the experiments as shown in Fig. 4.

### Effect of the number of load repetition

The second factor considered was the number of load repetitions. In the test were used 1, 3, 5, 9, 15 unloading cycles with the constant load amplitudes between the specified upper limits and zero. The seismic design load of prestressed concrete member for buildings in Japan is corresponding to about 0.76 times the ultimate strength, assuming that the load factors are 1.2 for the dead and live loads and 1.5 for the seismic load. Under this design load, the compressive extreme fiber strains of beams is around 1.8%. Therefore, the load producing the strain of 1.8% in the compressive extreme fiber of test beam by the virginal loading was repeated by the specified number of repetitions and, afterwards, monotonous increasing load was applied to failure. In one series of test, specimens had neither stirrups nor erection reinforcements except the prestressing steel itself. Another series of test, specimens had the standard stirrups described before and 2- $\phi$ 9 mm and 2- $\phi$ 6 mm axial erection reinforcing bars each in compression and tension side of the section respectively. The reduction in strength was not appreciable even after 15 cycles of loading. The ductilities of the specimens with ordinary reinforcements tended to increase with the increasing number of loading cycles, whereas those without ordinary reinforcements decreased after 9 repetition of loading. Based on the simplified stiffness degradation-moment relationship of the tested specimens with and without reinforcements respectively, the degradations of stiffnesses were plotted against the number of loading cycles as shown in Fig. 5.

## TEST RESULTS UNDER THE REVERSED REPEATED LOADS

Secondly, the transient flexural behaviors under the reversed repeated load were investigated. Effect of the auxiliary ordinary reinforcements. In this series, the test specimens were made from the similar materials. But the prestressing tendon was located in the centroid of the section. Transferred prestress was one-sixth the compressive strength of concrete. The amounts of the longitu-

dinal non-tensioned ordinary reinforcements were 2- $\phi$ 13 mm in the compression and tension sides of the section. Moreover, both types of test beams with and without stirrups of  $\phi$ 6 mm at the intervals of 25mm were prepared. The variety of the section details of tested beams is shown in Fig. 6.

At first about 90% of the theoretical capacities of beams were applied then fully reversed repeated loadings were performed. The applied loads were unloaded when the moment-curvature curve in each cycle reached the envelope curve. Other test conditions were almost the same as those in the prescribed test result. Fig. 6 shows parts of the envelope curve of the moment-curvature relations where the values of moment and curvature are divided by the ultimate ones theoretically obtained under the monotonous loading condition. For the test beams APG-46 and-48 without any stirrups the reduction in flexural capacities is remarkable although the ductility increases to some extent. The test beam APG-49 with 2- $\phi$ 13 mm compressive and tensile reinforcement and 2- $\phi$ 6 mm stirrups spaced by 25 mm showed a considerable potential energy to resist the heavy repeated over-load. The stiffness reduction and the ductility at the peak condition during the load repetition are shown in Fig. 7.

#### Effects of the eccentricity of tendons and the curvature amplitudes

In conventional design of prestressed concrete structures, the eccentricities of the prestressing steel along the member axis are usually determined in proportion to the moment distribution due to the dead and live loads. Therefore, the prestressed concrete beam in the rigid portal frame as shown in Fig. 8 has the different moment-curvature properties in every section along its axis. For the estimation of the entire deformation of such member, it is necessary to obtain the effect of the eccentricity of the prestressing tendon on the moment-curvature relation. Some experimental results on this problem under repeated over-load are described. The tests were composed of the following three series;

- (1) the beams with the same eccentricity -  $h/6$  of the prestressing steel were tested under the three kinds of the constant curvature amplitudes, i.e. level 1, 2 and 3, which corresponded to 1.0, 0.8 and 0.5 times the theoretical ultimate moment of the beams under monotonous loading respectively,
- (2) the beams with the five kinds of the eccentricities ranging from  $-h/6$  to  $+h/6$  were tested under the constant curvature amplitude corresponding to the theoretical ultimate moment of the beams,
- (3) the beams with the section A to E as shown in Fig. 8 were tested under the constant curvature amplitudes, simulating the maximum moment distribution of steady state under horizontal seismic action.

Alphabetical symbol and two digital numbers of the name of test beams show the eccentricities of the tendon and the applied curvature amplitudes in both directions. Except the eccentricities of the tendon test beams had the similar properties as used in the preceding experiments under the non-reversed repeated loads. Parts of the obtained moment-curvature relationships are shown in Fig. 9. In order to realize the trend of the mechanical deterioration the representative coefficients in the idealized moment-curvature relationships shown in Fig. 10 are adopted. Fig. 11 shows the changes of such coefficients against the load repetition number  $N$ .

## SUMMARY

Flexural behaviors of prestressed synthetic lightweight aggregate concrete beams under repeated over-load are experimentally investigated. The factors considered in the test programs are the effects of the load intensity, the number of load repetition, the auxiliary ordinary reinforcements, the modes of repeated load and the eccentricities of the prestressing tendons.

## RESUME

On étudie le comportement à la flexion de poutres en béton à agrégats synthétiques légers précontraintes soumises à des surcharges répétées. Les facteurs considérés dans les programmes d'essais sont: les effets de la grandeur de la charge, le nombre de cycles de charges, les armatures auxiliaires normales, le type de charge répétée et l'excentricité des câbles de précontrainte.

## ZUSAMMENFASSUNG

Es wurde das Biegeverhalten vorgespannter Leichtbetonbalken unter wiederholter Ueberbelastung experimentell untersucht. Die im Testprogramm berücksichtigten Faktoren sind die Effekte der Belastungsgrösse, der Anzahl der Last-Wiederholungen, die zusätzliche übliche Bewehrung, die Art der wiederholten Last und die Exzentrizität der Spannkabel.

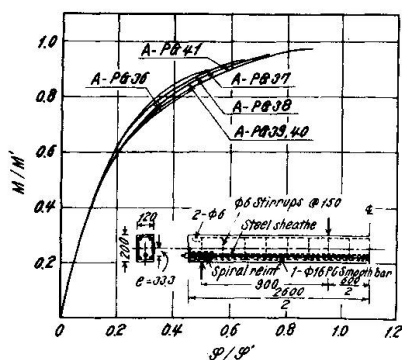


Fig. 1(a) Non-dimensional moment-curvature curves during loading stage (Unit of specimen dimensions in mm).

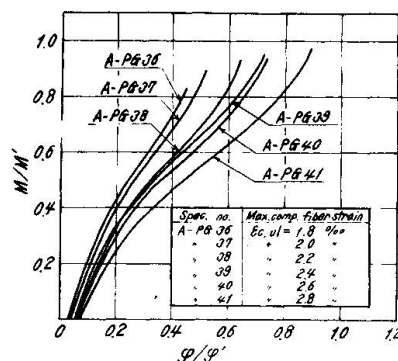


Fig. 1(b) Non-dimensional moment-curvature curves during unloading stage from various load levels.

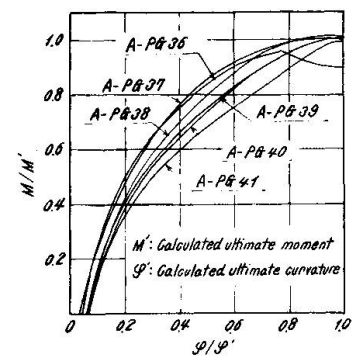


Fig. 1(c) Non dimensional moment-curvature curves during reloading stage after complete unload.

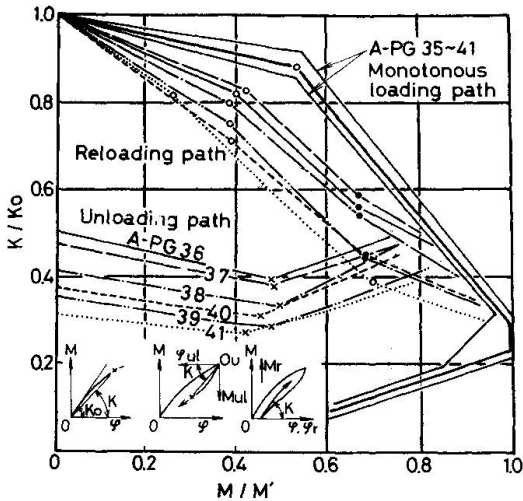


Fig. 2 Bi- or tri-linear approximation of flexural moment-stiffness relations under repeated over-load with various load levels.

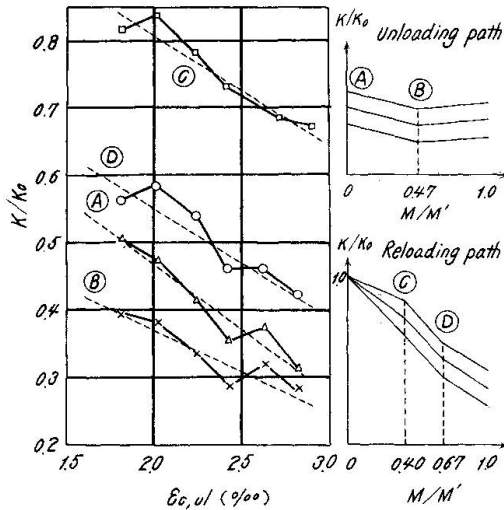


Fig. 3 Degrading flexural stiffness  $K/K_0$  against the compressive extreme fiber strain  $\epsilon_{c,ul}$  of concrete at the beginning of unloading.

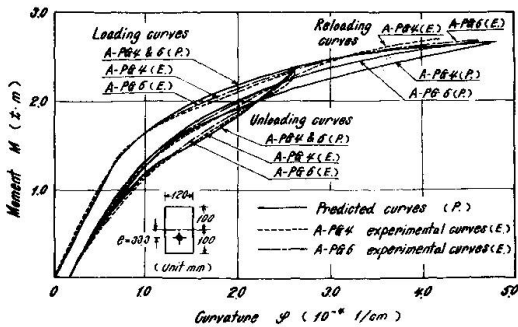


Fig. 4 Prediction of moment-curvature curves of prestressed concrete beams under repeated loadings.

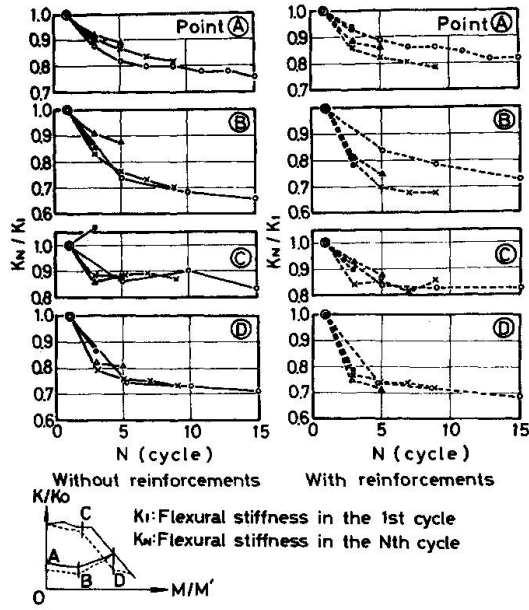


Fig. 5 Degrading flexural stiffness  $K_w/K_i$  against the load number.

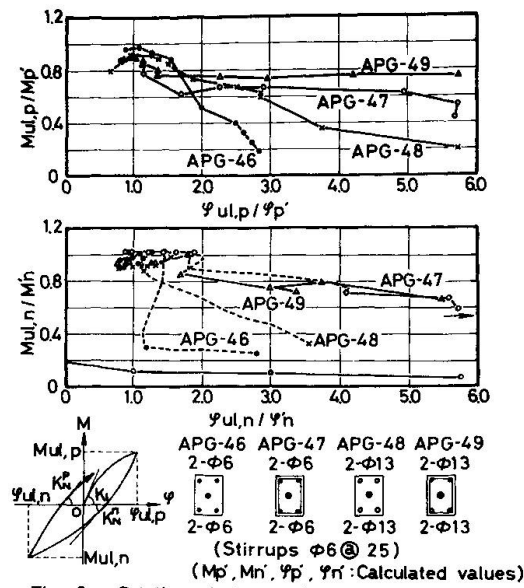


Fig. 6 Relations between the moment and curvature at the instant of unloading under full reversed repeated overload.

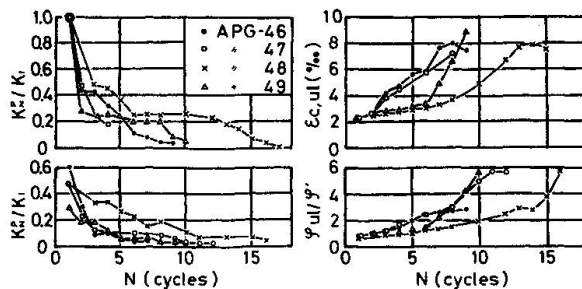


Fig. 7 Degrading of flexural stiffness  $K_w/K_i$ , and development of compressive extreme fiber strain  $\epsilon_{c,ul}$  of concrete and ductility factor  $\psi_{ul}/\psi_p'$  at the peak load against the load number.

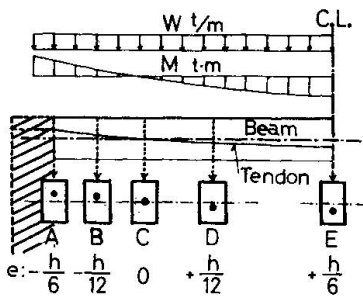


Fig. 8 Tendon profile of prestressed concrete beam in a rigid frame. (e: eccentricities.)

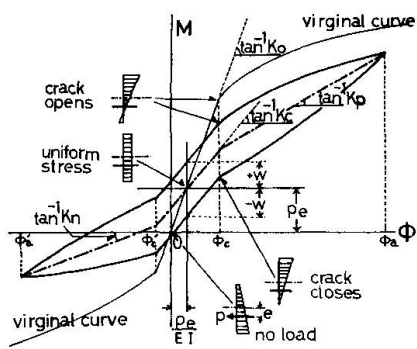


Fig. 10 Proposed model of N-th cycle moment-curvature curve of prestressed concrete beam under reversed flexural loading. ( $\phi_c$ ,  $\phi_c'$ : specified constant curvature amplitudes)

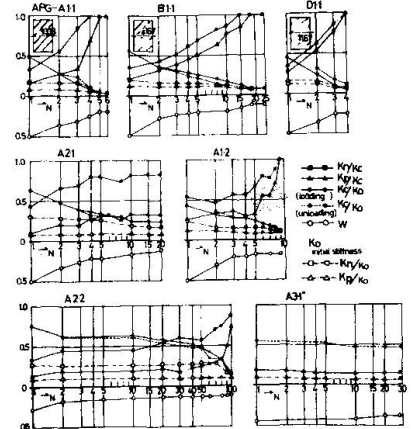


Fig. 11 Changes of representative coefficients of the moment-curvature model against the load repetition number N.

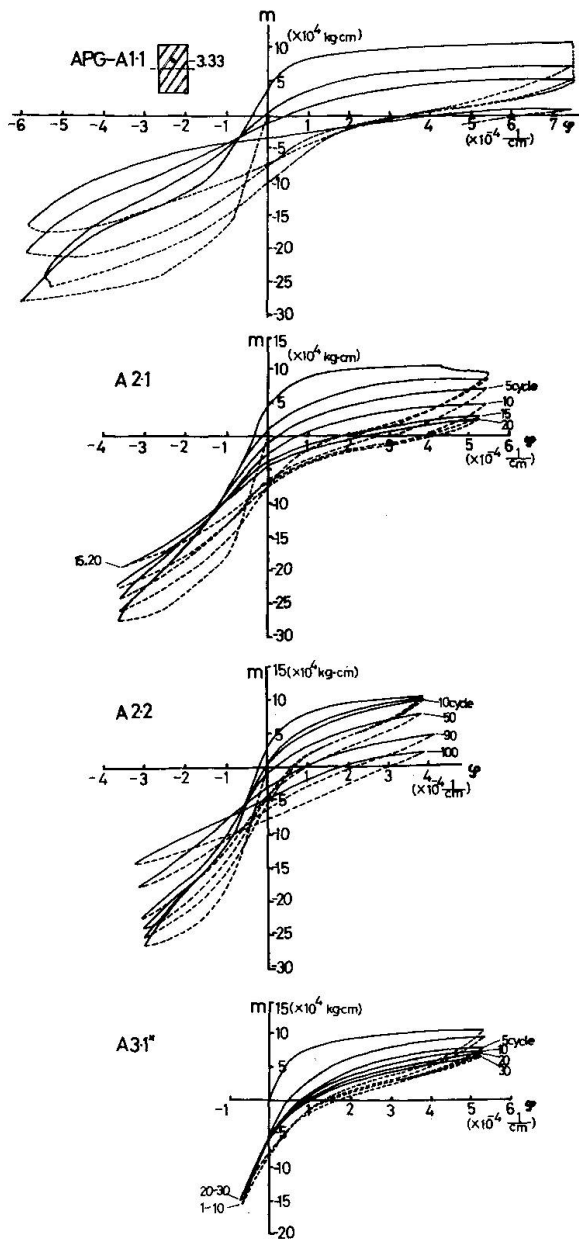


Fig. 9 A part of the experimental m- $\phi$  curves.

